frontiers | Frontiers in Neuroscience

TYPE Original Research
PUBLISHED 03 July 2023
DOI 10.3389/fnins.2023.1148683

OPEN ACCESS

EDITED BY
Jian-Huan Chen,
Jiangnan University, China

REVIEWED BY
Sheng Zhong,
Sun Yat-sen University Cancer Center, China
Alfredo Gonzalez-Sulser,
University of Edinburgh, United Kingdom

*CORRESPONDENCE
Yann Herault
✉ herault@igbmc.fr

RECEIVED 20 January 2023
ACCEPTED 02 May 2023
PUBLISHED 03 July 2023

CITATION
Martin Lorenzo S, Muniz Moreno MDM, Atas H, Pellen M, Nalesso V, Raffelsberger W, Prevost G, Lindner L, Birling M-C, Menoret S, Tesson L, Negroni L, Concordet J-P, Anegon I and Herault Y (2023) Changes in social behavior with MAPK2 and KCTD13/CUL3 pathways alterations in two new outbred rat models for the 16p11.2 syndromes with autism spectrum disorders.
Front. Neurosci. 17:1148683.
doi: 10.3389/fnins.2023.1148683

Changes in social behavior with MAPK2 and KCTD13/CUL3 pathways alterations in two new outbred rat models for the 16p11.2 syndromes with autism spectrum disorders

Sandra Martin Lorenzo[1], Maria del Mar Muniz Moreno[1], Helin Atas[1], Marion Pellen[1], Valérie Nalesso[1], Wolfgang Raffelsberger[1], Geraldine Prevost[2], Loic Lindner[2], Marie-Christine Birling[2], Séverine Menoret[3,4], Laurent Tesson[4], Luc Negroni[1], Jean-Paul Concordet[5], Ignacio Anegon[4] and Yann Herault[1,2]*

[1]Université de Strasbourg, CNRS UMR7104, INSERM U1258, Institut de Génétique et de Biologie Moléculaire et Cellulaire, Illkirch, France, [2]Université de Strasbourg, CNRS, INSERM, CELPHEDIA-PHENOMIN, Institut Clinique de la Souris, Illkirch, France, [3]Nantes Université, CHU Nantes, INSERM, CNRS, SFR Santé, Inserm UMS 016 CNRS UMS 3556, Nantes, France, [4]INSERM, Centre de Recherche en Transplantation et Immunologie UMR1064, Nantes Université, Nantes, France, [5]MNHN, CNRS UMR 7196/INSERM U1154, Sorbonne Universités, Paris, France

Copy number variations (CNVs) of the human 16p11.2 locus are associated with several developmental/neurocognitive syndromes. Particularly, deletion and duplication of this genetic interval are found in patients with autism spectrum disorders, intellectual disability and other psychiatric traits. The high gene density associated with the region and the strong phenotypic variability of incomplete penetrance, make the study of the 16p11.2 syndromes extremely complex. To systematically study the effect of 16p11.2 CNVs and identify candidate genes and molecular mechanisms involved in the pathophysiology, mouse models were generated previously and showed learning and memory, and to some extent social deficits. To go further in understanding the social deficits caused by 16p11.2 syndromes, we engineered deletion and duplication of the homologous region to the human 16p11.2 genetic interval in two rat outbred strains, Sprague Dawley (SD) and Long Evans (LE). The 16p11.2 rat models displayed convergent defects in social behavior and in the novel object test in male carriers from both genetic backgrounds. Interestingly major pathways affecting MAPK1 and CUL3 were found altered in the rat 16p11.2 models with additional changes in males compared to females. Altogether, the consequences of the 16p11.2 genetic region dosage on social behavior are now found in three different species: humans, mice and rats. In addition, the rat models pointed to sexual dimorphism with lower severity of phenotypes in rat females compared to male mutants. This phenomenon is also observed in humans. We are convinced that the two rat models will be key to further investigating social behavior and understanding the brain mechanisms and specific brain regions that are key to controlling social behavior.

KEYWORDS

copy number variation, neurodevelopment, intellectual disability, autism spectrum disorders, rat model, social behavior, recognition memory

1. Introduction

The 16p11.2 locus is a pericentromeric region found in chromosome 16, one of the most gene-rich chromosomes in our genome, for which 10% of its sequence consists of segmental duplications (Redaelli et al., 2019). These elements give strong instability and induce the appearance of copy number variations (CNV) because of the recurrent non-allelic homologous recombination mechanism (Hastings et al., 2009). The most prevalent rearrangement, deletion and duplication are generated between two low copy repeats (LCR), named BP4 and BP5, and encompasses 600 kb. 16p11.2 CNVs are an important risk factor for neurodevelopmental disorders (Torres et al., 2016), including intellectual disability (ID; Cooper et al., 2011) and autism spectrum disorder (ASD; Marshall et al., 2008; Weiss et al., 2008; Fernandez et al., 2010; Sanders et al., 2011; Steinman et al., 2016). In addition, the deletion and duplication of 16p11.2 have been linked to epilepsy (Shinawi et al., 2010; Zufferey et al., 2012; Reinthaler et al., 2014) and attention deficit hyperactivity disorder (ADHD; Angelakos et al., 2017), whereas only the duplication has been related to schizophrenia, bipolar disorder and depression (McCarthy et al., 2009; Rees et al., 2014; Steinberg et al., 2014; Drakesmith et al., 2019).

Besides, these chromosomal rearrangements have been linked to mirrored physical phenotypic effects. The 16p11.2 deletion has been associated with the risk of diabetes-independent morbid obesity and large head circumference, while the 16p11.2 duplication has been associated with low body mass index (BMI) and small head circumference (Walters et al., 2010; Jacquemont et al., 2011; Zufferey et al., 2012; D'Angelo et al., 2016). Considering this reciprocal impact on BMI and head size, it has been suggested that changes in gene transcript levels could be responsible for the symptoms associated with these CNVs. More importantly, the severity of the developmental delay and other comorbidities vary significantly in the human population with some people having an ASD or IQ below 70 and others just below average (D'Angelo et al., 2016; Chawner et al., 2021; Benedetti et al., 2022).

Animal models have been developed and characterized to investigate the interplay between genes and proteins, the consequences on brain activity and behavior and the understanding of neurocognitive processes affected in humans. Genes of the 16p11.2 region are highly conserved on mouse chromosome 7 and several mouse models for the deletion or duplication of the 16p11.2 homologous region have been generated (Horev et al., 2011; Portmann et al., 2014; Arbogast et al., 2016; Benedetti et al., 2022). Among them, our novel 16p11.2 CNV mouse models in pure C57BL/6 N genetic background named *Del(7Sult1a1-Spn)6Yah* (noted Del/+) and *Dp(7Sult1a1-Spn)6Yah* (noted Dup/+) and investigated them focusing on behavior and metabolism (Arbogast et al., 2016). We found that *Sult1a1-Spn* CNVs affect growth, weight, adiposity, activity and memory in opposite ways. Mice carrying the deletion showed weight and adipogenesis deficits, hyperactivity with increased stereotypic behavior and novel object memory impairments. Instead, mice carrying the duplication showed weight and adipogenesis increase, hypo-activity and memory improvements. We also found that the genetic background can favor the social interaction deficits in the deletion mice model. Altogether this observation suggests that this deficit could be the consequence of the genetic context.

To generate a model presenting more suitable autistic traits, we engineered the deletion or duplication of the human homologous region 16p11.2 in the rat in two different outbred genetic backgrounds. As a model of human disease, the rat is a more sociable animal than the mouse with a large spectrum of similar and complementary behavioral assessments and the outbred genetic background, although representing a challenge, could be of interest to detect the most robust phenotypes. Rats have shown differences from mice in several models of human disease in which genetically engineered animals for the same genes have been generated. The main contribution of our research is the establishment and validation of two new 16p11.2 rat models that can be helpful to test novel pre-clinical pharmacological therapies targeting specific phenotypes and finally help to improve the lives of patients.

2. Materials and methods

2.1. Rat lines and genotyping

The 16p11.2 rearrangement, deletion and duplication, were studied in rat models engineered through CRISPR/Cas9 technology (Menoret et al., 2015) as detailed in the Supplementary material (Figure 1). Rat models were then bred and maintained in our animal facility which is accredited by the French Ministry for Superior Education and Research and the French Ministry of Agriculture (agreement #A67-218-37) following the Directive of the European Parliament: 2010/63/EU, revising/replacing Directive 86/609/EEC and the French Law (Decree n° 2013-118 01 and its supporting annexes entered into legislation on 01 February 2013) relative with the protection of animals used in scientific experimentation. All animal experiments were approved by the local ethical committees (Approval Committee: Com'Eth N°17 and French Ministry for Superior Education and Research (MESR) with approval licenses: internal numbers 2012-009 and 2014-024, and MESR: APAFIS#4789-2016040511578546) and supervised in compliance with the European Community guidelines for laboratory animal care and use and every effort was made to minimize the number of animals used and their suffering.

2.2. Behavioral analysis

To decipher more in detail alterations of specific cognitive functions and autistic traits in 16p11.2 CNVs rat models on two

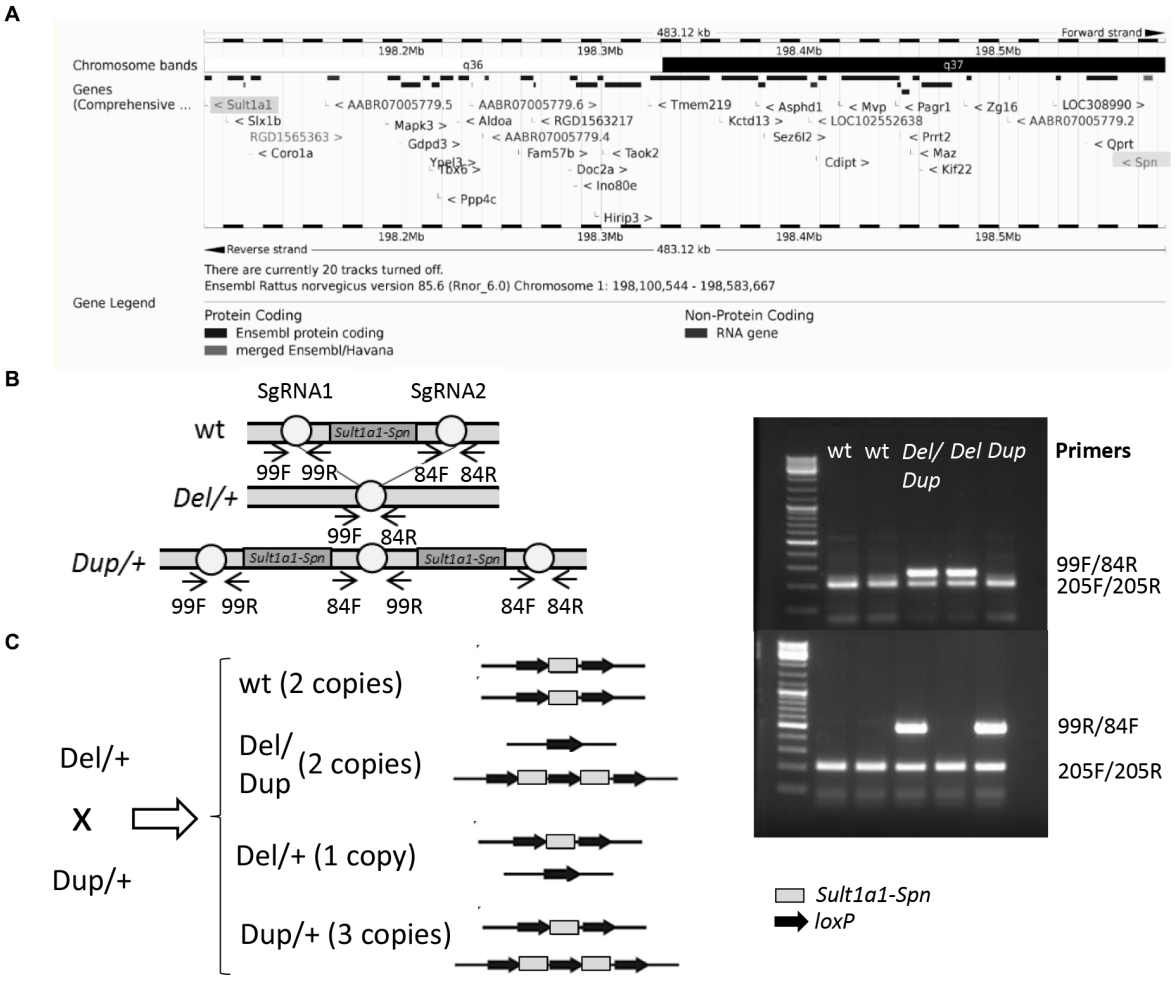

FIGURE 1
New rat SD model for the 16p11.2 syndromes. **(A)** The syntenic region 16p11.2 BP4-BP5 in the rat genome as represented in the UCSC database (Nassar et al., 2023). **(B)** Left: mutation strategy using CRISPR/Cas9 technology from the *in vitro* genome editing inside of a fertilized embryo and subsequent injection into a pseudo-pregnant female. We obtained individuals carrying the deletion and duplication of the *Sult1a1-Spn* region. Right: molecular validation. PCR-specific products for the wt (205 bp), *Del/+* (290 bp) and *Dup/+* (500 bp) alleles. **(C)** Breeding strategy for obtaining wt, *Del/+*, *Dup/+*, and *Del/Dup* littermates. **(D)** Junctions positions and details of the mutated genetic sequences for *Del* and *Dup* rat models. All genomic positions are given according to the UCSC rat genome browser (RGSC 6.0/rn6).

genetic backgrounds, Sprague–Dawley (SD) and Long Evans (LE), we evaluated several phenotypes with a validated rat phenotyping behavioral pipeline. We defined the protocol with tasks in which 16p11.2 mouse models showed robust phenotypes: alterations of exploration activity, object location and novel object recognition (NOR) memory, and social interaction. For SD 16p11.2 rat models, littermate animals from different crosses with four genotypes were used: wt, Del/+, Dup/+ and pseudo-disomic Del/Dup (Figure 1C). For LE 16p11.2 rat model, we used littermate animals from the wt and Del/+ cross to get mutant and control genotypes as littermates.

Behavioral studies were conducted in 14 to 16-week-old SD rats of both sexes separately, from 8 cohorts. Whereas LE rats were analyzed between 19 and 24 weeks old for both sexes separately, from 1 large cohort. Animals were housed in couples of 2 individuals per cage (Innocage Rat cages; 909 cm^2 of floor space; Innovive, San Diego, United States), where they had free access to water and autoclaved food (D04, Safe Diets, France). The temperature was maintained at

23°C ± 1°C and the light cycle was controlled as 12 h light and 12 h dark (light on at 7 a.m.).

On the testing days, animals were transferred to the experimental room antechambers 30 min before the start of the experiments. The body weight of the animals from the SD 16p11.2 rat models was recorded at 13 weeks old whereas the body weight of animals from LE 16p11.2 rat models was recorded at 2 weeks old, and followed at weaning and 19 weeks. All tests were scored blind to the genotype as recommended by the ARRIVE guidelines (Kilkenny et al., 2010; Karp et al., 2015). The protocols for open field, object location, object recognition memories and social interaction are described in the Supplementary material.

2.2.1. Open field

This test was used to study exploration activity. Rats were tested in an automated open field (90 × 90 × 39.5 cm) made of opaque PVC with black walls and floor (Imetronic, Pessac—France). The structure was equipped with infrared sensors for accurate location and rearing behaviors of the animal. An interface provided the formatting of signals from infrared sensors and allows communication with the computer, where the software POLY OPENFIELD v5.3.2 managed experimental data. The open field arena was divided into central and peripheral regions and was homogeneously illuminated at 15 Lux. Each animal was placed in the periphery of the open field and allowed to explore freely for 30 min. The distance traveled in the total arena and in each region of the arena, as well as, the number of rears were recorded over the test session.

2.2.2. Object location memory task

This test was based on the innate preference for the novelty showed by the rodents and it was carried out in the same open field arena as previously described. On the first day, rats were habituated to the arena for 15 min at 15 Lux. On the following day, animals were submitted to a first acquisition trial for 3 min in which they were individually placed in the presence of two identical objects A (syringe or flask for SD models and cup for LE model) located 15 cm away from one of the corners, on the northeast and northwest side of the box, respectively. In the case of the LE model, the test was refined by placing a reference band on the north wall of the open field. A 3-min retention trial (second trial) was conducted 5 min later, and then one of the familiar objects (right or left object) was displaced randomly to a novel location (B) on the south side. The exploration time of the two objects (when the animal's snout was directed toward the object at a distance ≤1 cm) was recorded during both trials. The minimum exploration time was set to 3 s, and rats that did not reach this criterion during the acquisition trial or retention trial were excluded from the study. We verified that no preference was seen during the exploration of the left and right objects. A recognition index (RI) was defined as $[(tB/(tA + tB)) \times 100]$. A RI of 50% corresponds to a chance level and a significantly higher RI reflects good recognition memory.

2.2.3. Novel object recognition memory task

This test allowed us to evaluate the ability to recognize previously encountered objects in murine models and like the Object location memory (OLM) task, this test is also based on the innate preference of rodents to explore novelty. We carried out Novel object recognition (NOR) in the same open-field arena as previously described.

Firstly, we developed the NOR test through a protocol based on the characterization of the mouse models, although we reduced the time of the trials to adapt the test to the intelligence of the rats. In the first 3 min acquisition trial, rats were presented with two identical objects A (syringe, block, bottle or flask). The animals from SD models that were evaluated in the NOR test did not belong to the same cohort as those that were analyzed in the OLM test, therefore the objects syringe and flask were never seen before the NOR test by these rats. A 3-min retention trial was conducted 3 h later. One of the two familiar objects was randomly changed for another novel object B. Test was analyzed for the OLM task.

The surprisingly good performance of the mutant individuals made us question the simplicity of this test for an intelligent animal like the rat. For this reason, we were motivated to develop a new NOR protocol.

In this case, animals from new cohorts were presented to three different objects located (A, B, C) at the northwest, northeast and southwest corner of the arena during the 3-min acquisition trial. A 3-min retention trial was conducted 3 h later. One of the three familiar objects was randomly changed for another novel object (D). The exploration time of the three objects (when the animal's snout was directed toward the object at a distance ≤1 cm) was recorded during both trials. The minimum exploration time was set to 3 s, and rats that did not reach this criterion during the acquisition trial or retention trial were excluded from the study. We verified that no particular object preference was seen during the exploration. A recognition index (RI) was defined as $[(tD/(tA + tB + tD)) \times 100]$. A RI of 33.3% corresponds to a chance level and a significantly higher RI reflects good recognition memory.

2.2.4. Social interaction task

This analysis focused on the evaluation of rat social behavior by manually scoring a battery of social interactions (Lorbach et al., 2018) among two animals of the same sex, age and genotype, housed in different cages. The test was carried out in a previously described standardized open-field arena during 10 min of video recording.

2.3. Statistical analysis

The statistical analysis of our results was carried out using standard statistical procedures operated by SigmaPlot software (Systat Software, San Jose, United States). All outliers were identified using Grubbs' test from calculator GraphPad (GraphPad Software, San Diego) or ROUT method with a Q value of 1% from GraphPad Prism 7.01 (Motulsky et al., 2006; GraphPad Software, San Diego) when data with nonlinear regression. Acquired data from the behavioral characterization of 16p11.2 rat models were analyzed using one-way ANOVA followed by Student's *t*-test and Tukey's *post hoc* test whenever data presented normal distribution and equal variance. Otherwise, we used the non-parametric Kruskal-Wallis one-way analysis of variance and the Mann–Whitney *U*-test. One sample t-test was used also to compare recognition index values to the set chance level (50%). The data to evaluate the mutant allele transmission was analyzed by a Person's Chi-squared test. Data are represented as the mean ± SEM and the statistically significant threshold was $p < 0.05$.

2.4. Transcriptomic analysis

Hippocampus from 4 Del/+ [noted as Del(16p11)], 5 Dup/+ [noted as Dup(16p11)] and 4 Del/Dup [noted as Del/Dup(16p11)] SD rats and 6 wt littermates for each, were isolated and flash frozen in liquid nitrogen. Total RNA was prepared using an RNA extraction kit (Qiagen, Venlo, Netherlands) according to the manufacturer's instructions. Samples quality was checked using an Agilent 2,100 Bioanalyzer (Agilent Technologies, Santa Clara, California, United States). All the procedures and the analysis are detailed in the Supplementary material.

The preparation of the libraries was done by using the TruSeq Stranded Total RNA Sample Preparation Guide—PN 15031048. The molecule extracted from the biological material was polyA+ RNA. The Whole genome expression sequencing was performed by the platform using Illumina Hiseq 4000 and generating single-end RNA-Seq reads of 50 bps length. The raw sequenced reads were aligned by Hisat2 against the Rno6.v96. 32,623 ENSEMBL Gene Ids were quantified aligning to the Rno6.v96 assembly. HTSeq-count was used to generate the raw counts. The downstream analyses were carried on with in-house bash scripts and R version 3.6 scripts using FCROS (Dembélé and Kastner, 2014) and DESeq2 (Love et al., 2014) packages to identify the DEGs. Raw reads and normalized counts have been deposited in GEO (Accession No. GSE225135).

We performed the functional differential analysis (Duchon et al., 2021) and grouped all the pathways into 25 functional categories (noted meta-pathways). Then, to assess the gene connectivity we build a minimum fully connected protein–protein interaction (PPI) network (noted MinPPINet) of genes known to be involved in all meta-pathways we defined as they were associated with each pathway via GO (Ashburner et al., 2000) and KEGG databases (Esling et al., 2015) and added regulatory information to build the final 16p11 dosage sensitive regulatory PPI network (noted RegPPINet). We used the betweenness centrality analysis to identify hubs, and keys for maintaining the network communication flow.

2.5. ddPCR analysis

Analyses were performed by Droplet Digital™ PCR (ddPCR™) technology. All experiments were performed following the previously published protocol (Lindner et al., 2021). Primers are described in Supplementary Table S1.

2.6. Identification of central genes linked to the behavioral phenotypes

To further study the genotype–phenotype relationship in those models we combined the behavioral results and the RNA-Seq data to identify central genes altered in the models linked to the observed phenotypes using the genotype–phenotype databases GO, KEGG and DisGeNET. For this, we combined the knowledge from the human disease database DIsGeNET and the GO genesets (see Supplementary material). Then we queried our RNA-Seq data for those genes to identify those found deregulated in the datasets. Table 1 summarized the results with the genes annotated with the expression level, regulation sense on each model, log2FC and standard deviation of the log2FC.

2.7. Proteomic analysis

Fresh entire hippocampal tissues were isolated by CO2 inhalation/dissection of naive rats and snap frozen. Then, lysed in ice-cold sonication buffer supplemented with Complete™ Protease Inhibitor Cocktail (Roche). Individual samples were disaggregated and centrifuged at 4°C for 30 min at 14000 rpm. Protein mixtures were TCA (Trichloroacetic acid/Acetone)-precipitated overnight at 4°C. Samples were then centrifuged at 14,000 rpm for 30 min at 4°C. Pellets were washed twice with 1 mL cold acetone and centrifuged at 14,000 rpm for 10 min at 4°C. Washed pellets were then urea-denatured with 8 M urea in Tris–HCl 0.1 mM, reduced with 5 mM

TABLE 1 Summary of the transcriptional analysis of the SD and LE 16p11.2 models.

Genetic background	Sprague Dawley			Long Evans		
Nb of annotated transcripts Rno6.v96	32,623					
Nb of expressed (EGs) genes	23,148					
Number of 16p11 homologous region genes [*Sult1a1-Spn*]	28					
Sexes		Male		Males	Female	Both
Genotype	Del/+	Dup/+	Del/Dup	Del/+		
Differentially expressed genes (DEG)						
Total identified by FCROS FDR < 0.05	966	1,367	1,071	1,068	1,324	1,544
Upregulated DEGs	508	719	640	613	531	737
Downregulated DEGs	458	648	431	455	793	807
Differential functional analysis (DFA)						
Number of GAGE KEGG and GOs (CC, BP, MF) terms misregulated in the model FDR < 0.1	146	68	5	248	100	31
Number of terms upregulated in the model FDR < 0.1	46	68	1	10	93	0
Number of terms downregulated in the model FDR < 0.1	100	0	4	238	7	31

TCEP for 30 min, and then alkylated with 10 mM iodoacetamide for 30 min in the dark. Both reduction and alkylation were performed at room temperature and under agitation (850 rpm). Double digestion was performed with endoproteinase Lys-C (Wako) at a ratio of 1/100 (enzyme/proteins) in 8 M urea for 4 h, followed by overnight modified trypsin digestion (Promega) at a ratio of 1/100 (enzyme/proteins) in 2 M urea. Both Lys-C and Trypsin digestions were performed at 37°C. Peptide mixtures were then desalted on a C18 spin-column and dried on Speed-Vacuum before LC-MS/MS analysis (see Supplementary material).

3. Results

3.1. General and behavioral characterization of the SD 16p11.2 rat models

The 16p11.2 region is conserved in the rat genome on chromosome 1 (Figure 1A). Using CRISPR/Cas9 we generated first the deletion and the duplication of the conserved interval containing *Sult1a1* and *Spn1* (Figures 1B,C) and we determined the precise sequence of the new borders of the deletion and duplication (Figure 1D).

To carry out the behavioral analysis of the SD 16p11.2 rat models we combined the deletion (*Del*/+) and the duplication (Dup/+) for the generation of 4 groups of genotypes: wt control, Del/Dup pseudo-disomic for the 16p11.2 conserved region, Del/+ and Dup/+ littermates (Figure 1C). Before testing, we checked the transmission of the alleles and we did not find any deviation from Mendelian rate (Supplementary Table S2). Then, we analyzed the effect of 16p11.2 CNVs on the weight of the 13 weeks old rats. We observed that male rats carrying 16p11.2 deletion showed a decrease in body weight compared to wt littermates, while males carrying 16p11.2 duplication did not show alterations compared to wt littermates (Figure 2A). The 16p11.2 rearrangements did not affect the body weight of female rats (Figure 2A).

As a first analysis for consequences of 16p11.2 CNVs in neuronal function, we measured spontaneous locomotion activity and exploratory behavior in the open field test (Supplementary Table S4). The horizontal activity was measured through total traveled distance, whereas the vertical activity was analyzed by the number of rears. As shown in Figure 2B, increased variability was observed in the distance traveled and the rearing activity. The only significant differences were found between extreme genotype male Del/+ vs. Dup/+ and between female Del/Dup vs. Dup/+ for both the distance traveled and the rearing activity in the open field.

Then, we carried out the novel object location recognition test and the novel object recognition test, common assays for assessing impaired memory in rodents. For the novel object location recognition, animals were challenged to discriminate a moved object from an unmoved object. We first evaluated the performances of males and females separately, and as no significant sex differences were noted, we combined these data across both sexes. No difference was observed between genotypes in the retention session [Kruskal-Wallis one-way analysis of variance: $H_{(3)} = 5.61$; $p = 0.132$; Supplementary Figure S1A]. We also compared the recognition index of the animals, i.e., the percentage of exploration time of the new object location, with the level of chance (50%). The new object position was always explored more than the object not moved for all the genotypes.

Following these observations, we next assessed novel object recognition from a first paradigm, based on the protocol used for the CNVs 16p11.2 *Sult1a1-Spn* mouse model. The animals should be able to differentiate an object observed previously during the acquisition phase from a novel object presented during the retention phase (Supplementary Figure S1B). All four genotypes engaged in similar levels of novelty discrimination [One way ANOVA: $F_{(3,88)} = 0.038$; $p = 0.99$]. We also compared the recognition index with the level of chance (50%). A general preference was observed for the new object compared to the familiar object. The rat 16p11.2 models displayed correct recognition memory, with an increased time of the new object exploration spent by rats compared to mice (Arbogast et al., 2016).

Thus, we used a more complex object recognition paradigm with 3 different objects (Supplementary Figure S1C). In this case, the male Del/+ carriers showed impairment in the discrimination of the novel object compared to all the other genotypes (Figure 2C). Nevertheless, no alteration was observed in the females, with all the genotypes able to discriminate the novel vs. the two familiar objects.

Finally, the last task focused on studying rat social interactions by analyzing different social behavior (Lorbach et al., 2018; Figure 2D). The Del/+ male displayed significantly increased time in solitary compared to all genotypes. In addition, 16p11.2 Del/+ was associated with the presence of more pinning, a behavior to exert dominance. Interestingly the pinning behavior was found also in the Del/Dup male animals. Furthermore, male Dup/+ showed increased agnostic behavior compared to all genotypes. Surprisingly we did not see any social phenotypes in females of the Del/+ or Dup/+ genotype.

3.2. Behavioral characterization of the LE *Del/+* 16p11.2 rat model

Elucidating the genetic mechanisms by which some CNVs influence neurodevelopment requires a rigorous quantitative analysis of the human phenotype but also the establishment of validated model systems in which the phenotypic diversity is conserved. Based on previous results obtained on a pure inbreed mouse C57BL/6JN, or on a mixed B6.C3H genetic background (Arbogast et al., 2016) and now on a rat outbred SD model, we decided to investigate if the phenotypes were robust enough, and the deficits preserved in a different background. In addition, we considered it pertinent to verify if the females were equally more resilient to the deletion of the 16p11.2 region than the males in this new genetic background. For this purpose, we engineered the deletion of the homologous region to the human 16p11.2 BP4-BP5 locus in a rat LE outbred strain and we verified the location of the specific Del interval (Supplementary Figure S2). Interestingly the transmission of the Del/+ allele was affected in females of the LE 16p11.2 model (Supplementary Table S1) while males did not show any significant change. We also evaluated the body weight of this new model for both sexes and found that the deletion of the 16p11.2 region caused a decrease in the body weight on the LE genetic background in both sexes (Figure 3A). Then, we proceeded to study the behavior using the same battery of behavioral tests (Supplementary Table S4). We analyzed the locomotion and exploratory activity of our second

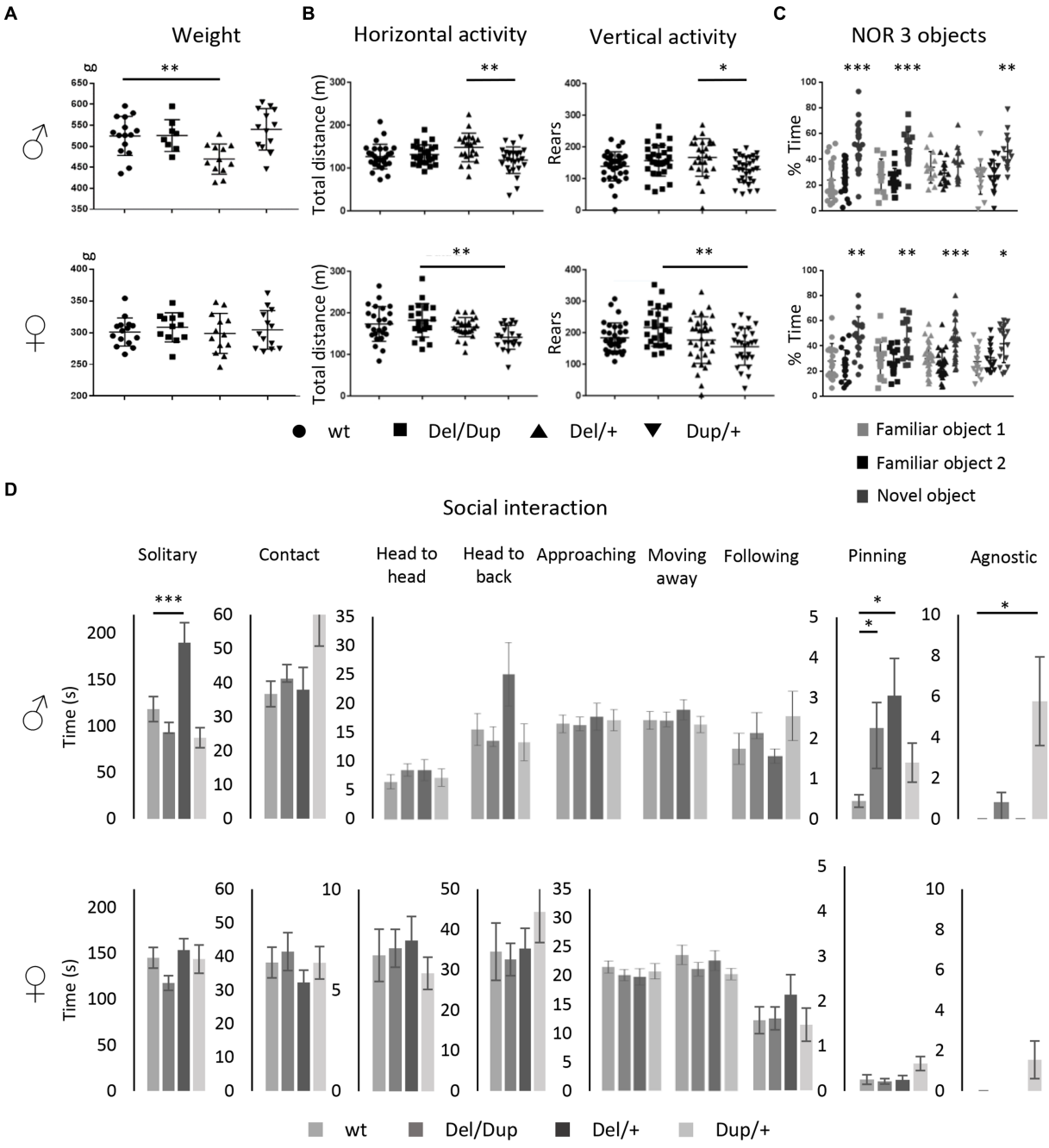

FIGURE 2
Phenotypic characterization of the 16p11.2 rat models on the SD genetic background. **(A)** Effects of *Sult1a1-Spn* rearrangements on body weight. Body Weight (g) of the 13 weeks old males [wt (n=15), *Del/Dup* (n=8), *Del/+* (n=12), and *Dup/+* (n=13)] and female rats [wt (n=15), *Del/Dup* (n=12), *Del/+* (n=13), and *Dup/+* (n=13)] from Del-Dup littermates. Only the deletion of 16p11.2 region caused reduced body weight in males [One way ANOVA between groups, $F_{(3,44)}$=6.24; p=0.001; Student t-test, *Del/+* vs. wt: $t_{(25)}$=3.39 p=0.002]. **(B)** Exploratory behavior of the rat 16p11.2 models in the open field test. Male [wt (n=28), *Del/Dup* (n=26), *Del/+* (n=21), and *Dup/+* (n=27)] and female [wt (n=25), *Del/Dup* (n=22), *Del/+* (n=26), and *Dup/+* (n=22)] rats were placed in the open field for 30min to explore the new environment. The horizontal activity was measured by the total distance traveled and vertical activity was recorded with the number of rears. Animals showed large variability and limited changes between genotypes except for *Del/+* vs. *Dup/+* male [One way ANOVA between groups, Total distance: $F_{(3,98)}$=4.33; p=0.007; Tukey's *post hoc* tests: *Del/+* vs. *Dup/+*: p=0.004; Rears: $F_{(3,117)}$=3.55; p=0.017; Tukey's *post hoc* tests: *Del/+* vs. *Dup/+*: p=0.016] and *Del/Dup* vs. *Dup/+* female [Kruskal-Wallis one-way analysis of variance, Total distance: $H_{(3)}$=14.18; p=0.003, Mann–Whitney Test: *Del/Dup* vs. *Dup/+*: p=0.002]; [One way ANOVA between groups, Rears: $F_{(3,116)}$=4.83; p=0.003; Tukey's *post hoc* tests: *Del/Dup* vs. *Dup/+*: p=0.002]. **(C)** Novel object recognition memory task of the rat 16p11.2 models after 3 h of retention with 3 objects. Male rats from different genotypes [wt (n=26), *Del/Dup* (n=16), *Del/+* (n=14) and *Dup/+* (n=16)] and female rats [wt (n=18), *Del/Dup* (n=16), *Del/+* (n=26), and *Dup/+* (n=17)] were tested for the novelty recognition. The graphs show the percentage of time spent by the animals exploring a novel object compared to the time spent exploring two familiar objects. We compared the recognition index, like the percentage of exploration time of the new object, to the level of chance (33.3%). Only the *Del/+* males showed impairment in the recognition index [One sample t-test: wt ($t_{(25)}$=4.6; p=0.0001), *Del/Dup* ($t_{(15)}$=2.82; p=0.01), *Del/+* ($t_{(13)}$=0.34; p=0.74) and *Dup/+* ($t_{(14)}$=3.58; p=0.0030)] compared to all the other genotypes in males and females. Surprisingly, no change was observed in the *Del/+* females [One sample t-test: wt ($t_{(17)}$=3.67; p=0.002), *Del/Dup* ($t_{(16)}$=3.08; p=0.01), *Del/+* ($t_{(25)}$=3.83; p=0.0008) and *Dup/+* ($t_{(16)}$=2.3; p=0.035)]. **(D)** Social interaction of the 16p11.2 rat models. Male [wt (n=15), *Del/Dup* (n=14), 16p11.2

(Continued)

FIGURE 2 (Continued)

Del/+ (n=10) and *Dup/+* (n=14)] and female [wt (n=14), 16p11.2 *Del/+* (n=15), 16p11.2 *Dup/+* (n=12) and *Del/Dup* (n=15)] rats were tested for impairment of social interaction in pairs of individuals from different home cages with the same genotype. The *Del/+* male rat showed increased solitary time [One way ANOVA between groups, Solitary behavior: $F_{(3,49)}$=9.85; p<0.001; Tukey's *post hoc* tests: *Del/+* vs. wt: p<0.001, *Del/+* vs. *Del/Dup*: p<0.001 and *Del/+* vs. *Dup/+*: p=0.005]. and pinning behavior with *Del/Dup* [Kruskal-Wallis one-way analysis of variance $H_{(3)}$=8.66; p=0.03; Mann-Whitney test: *Del/+* vs. wt: p=0.04; *Del/Dup* vs. wt: p=0.01] while Dup/+ males are more agnostic [Kruskal-Wallis one-way analysis of variance: $H_{(3)}$=13.63; p=0.003; Mann-Whitney test: *Dup/+* vs. wt: p=0.01; *Dup/+* vs. *Del/+*: p=0.02]. No altered social behavior has been detected in females (*p<0.05; **p<0.01; ***p<0.001).

model. First, we observed a reduction in the variability between the data of each individual regarding the results observed in the SD model. In addition, we detected a significant increase in horizontal activity among individuals carrying the 16p11.2 region deletion for both sexes. Finally, the Open Field test showed a significant increase in vertical activity, evaluated as the total number of rears, only in male rats. These results translate into the presence of stereotypical behaviors in this model associated with genotype and sex (Figure 3B).

Next, we performed the object location memory test (Supplementary Figure S3A; Supplementary Table S4). Our objective was to confirm, as in the case of the SD model, that the deletion of a copy of the 16p11.2 region has no impact on the object location memory in our second rat model. Considering that the 3-object discrimination protocol for the NOR test was the most appropriate, we decided to test the LE model (Supplementary Figure S3B; Figure 3C). Thus, this task showed that male mutant individuals, unlike control individuals, did not show an exploration preference for the new object. Furthermore, the object recognition index of these animals is not significantly higher than 33.3%. Instead, females carrying the 16p11.2 deletion on LE background did not develop any disorder in object recognition memory, showing a recognition index higher than the 33.3% chance level.

To get an animal model more relevant to autism with robust social behavior phenotypes shared among genetic backgrounds, we evaluated the LE model during the social interaction test (Figure 3D). Among the most interesting observations, we found that male mutant individuals spent significantly more time alone than control individuals. This phenotype was also observed in the SD 16p11.2 deletion model (Figure 2D). In addition, curiously, we discovered that these animals spent more time approaching their partner and we did not detect cases of pinning or agnostic behavior. In the case of LE females, the deletion of the 16p11.2 region had no effect on the development of social phenotypes for the evaluated events, as observed for the mutant SD females Overall the behavior results we identified were robust, as were observed similarly in the LE background to those obtained from the SD background in the 16p11.2 Del/+ model.

3.3. Expression analysis shed light on the pathways altered by a genetic dosage of the 16p11.2 homologous region

We investigated the gene expression profile of Del/+ and Dup/+ 16p11.2 male SD rat hippocampi by RNA-seq. After performing the DEA analysis using FCROS we identified 966 and 1,367 genes dysregulated (DEGs) in Del and Dup models, respectively (Table 1). Using those DEGs, we computed a PCA to assure the profile of expression of the DEGs could cluster our samples by their different gene dosage (Figure 4A). Additionally, to assure the quality of our data, we looked at the Euclidian distance between samples, calculated using the 28 genes susceptible of the dosage effect of the 16p11 region, and indeed all cluster by genotype (Figure 4B). Moreover, most of the genes of the region are following the gene dosage on the models. Looking at the FC profile across the region in the duplication, we found one gene with decreased FC expression LOC102552638, and several highly expressed genes as *Gdpd3*, two rat-specific *ABR07005778.1, AABR07005779.7*, and *Zg16*. Interestingly, in the deletion, we found 2 genes with an unpredicted increased expression, one outside of the region *RF00026,* possibly due to a bordering effect and another inside the region, *Zg16*. Overall, the gene expression dysregulation was corroborating the genetic dosage for this region in the different models (Figure 4C).

Looking at the expression of DEGs in both models, only 51% were strongly correlated to gene dosage (Figure 4D; Supplementary Table S5). Many genes of the 16p11 region (*AldoA, Mapk3, Cdipt, Coroa1, Kctd13, Ino80e, Mvp, Slx1b* and *Ppp4c*) showed a level of expression in RNA-Seq following a gene dosage effect that was confirmed by ddPCR (Supplementary Figure S4). Then, we wondered whose genome-wide DEG expression levels were positively, or negatively, correlated with the gene dosage. To answer this question, we fit a linear model considering CNVs as follows [lm(log2FC ~ CNV) == y ~ (b0 + b1*CNV)]. We found six genes of the region following a positive gene dosage effect *Aldoa, Sez6l2, Bola2, Kif22, Rad21l1, Ptx3, and Mael* with another gene, named *Chad*, out of the region, and presenting a negative correlation in the dosage model (Supplementary Table S5). Overall, 267 DEGs were commonly dysregulated in the Del/+ and Dup/+ models (19.7% shared DEGs of the total Dup/+ DEGs or 28.1% of the total Del/+ DEGs). Of those common 267 DEGS between models, 100 DEGs were downregulated in both models and 120 upregulated in both. Therefore, some functionalities should be commonly altered independently of the dosage. Nevertheless, 39 DEGs were following the region dosage effect (upregulated in the Dup/+ and downregulated in the Del/+), including the genes on the interval *Coroa1-Spn* and others like *Fam57b, Rad21l1, Mael, Ptx3* or *Rnf151,* found elsewhere in the genome, and 47 genes were altered in opposing regulatory sense. In particular, a few DEGs were following a negative dosage correlation such as *Cd8a, Evpl, Ucp3, Lipm* and *Cdh1* being upregulated in the Del/+ and downregulated in the Dup/+ (Figure 4E).

To go further, we performed the differential functional analysis (DFA) using gage (Luo et al., 2009). We found 146 and 68 pathways altered in the hippocampi of Del/+ and Dup/+ models, respectively. No downregulated pathway was found in the Dup/+ model whereas both up and downregulated pathways were found in the Del/+ hippocampi. After grouping the pathways inside of functionality-based defined meta-pathways (Duchon et al., 2021; Figure 5A; Supplementary Table S6). Although in the Dup/+ model, there were

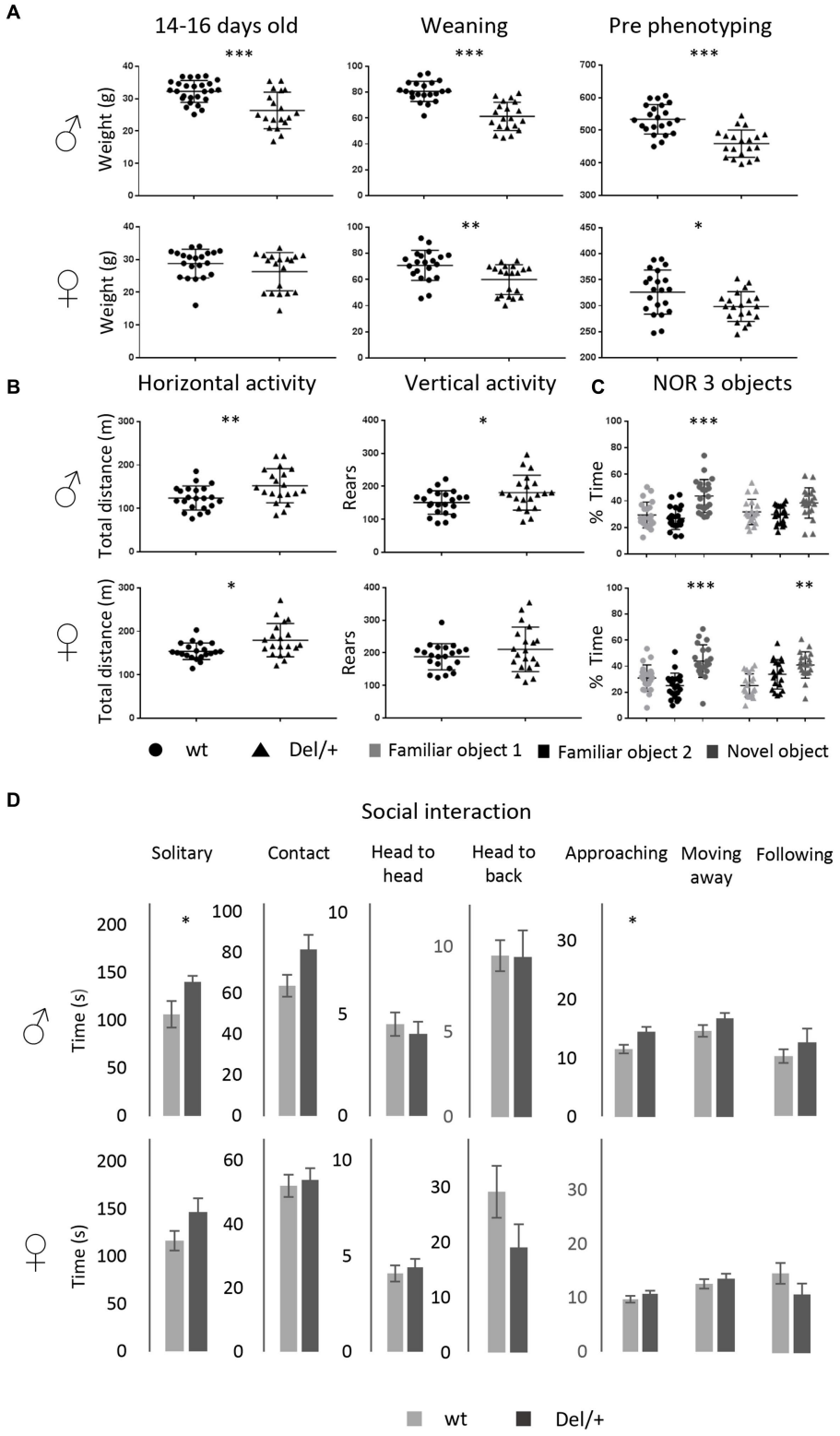

FIGURE 3
Phenotypic characterization of the 16p11.2 rat models on the LE genetic background. **(A)** Effects of *Sult1a1-Spn* deletion on body weight of LE 16p11.2 Del/+ rat model. Left: body weight (g) of the 14–16 days old males [wt (n=27) and Del/+ (n=19)] and female rats [wt (n=21) and Del/+ (n=19)]. Our observations showed a decreased body weight in Del/+ males compared to wt littermates [Student's t-test: $t_{(44)}$=3,819; p<0.001]. Central: body Weight at weaning of the males [wt (n=21) and Del/+ (n=20)] and female rats [wt (n=21) and Del/+ (n=20)] from LE Del/+ littermates. The deletion of the 16p11.2 region caused body weight decrease in male [Student's t-test $t_{(39)}$=6,550; p<0.001] and female individuals [Student's t-test $t_{(39)}$=3,036; p=0.004] compared to wt littermates. Right: body weight of 16p11.2 Del/+ male [wt (n=22) and Del/+ (n=20)] and female [wt (n=21) and Del/+ (n=20)] littermates during the first week of phenotype analysis. The male and female individuals carrying the deletion of the interest region continued to show a decrease in their body weight throughout their development [Student's t-test for males: $t_{(40)}$=5,550; p<0.001; Student's t-test for females: $t_{(39)}$=2,451;

(Continued)

FIGURE 3 (Continued)

p=0.019]. **(B)** Open Field test results illustrate the exploratory activity of the LE 16p11.2 rat model. Male [wt (n=22) and *Del/+* (n=20)] and female [wt (n=21) and Del/+ (n=20)] littermates were analyzed for horizontal and vertical activity. The 16p11.2 deletion caused increased horizontal activity in our model regardless of the sex of the animals [Student's t-test for males: $t_{(40)}$=−2,726; p=0,009; Mann–Whitney U Statistic for females: T=510,000; p=0.02]. However, the deletion of one copy of the interest region caused increased vertical activity only in male individuals [Student's t-test $t_{(40)}$=−2,174; p=0.036]. **(C)** The deletion of the 16p11.2 region causes a novel object recognition memory disorder in our rat model on LE genetic background. For the NOR test with 3 objects, the recognition index reflects the ability of rats to recognize the new object from the 2 familiar objects after a 3 h delay. Males mutant animals [wt (n=22) and Del/+ (n=20)] were impaired to recognize the new object when we compared the recognition index, like the percentage of exploration time of the new object, to the level of chance [33.3%; One sample t-test: wt ($t_{(21)}$=3.94; p=0.0008) and Del/+ ($t_{(19)}$=2.02; p=0.0569)]. However, the females of this model [wt (n=21) and Del/+ (n=20)] showed a preference for the new object that is reflected in a recognition index significantly higher than the level of chance [One sample t-test: wt ($t_{(20)}$=3.92; p=0.0008) and Del/+ ($t_{(19)}$=3.4; p=0.003)]. **(D)** Evaluation of the behavior of the LE 16p11.2 rat model in the social interaction test. The male [wt (n=11) and Del/+ (n=10)] and female [wt (n=10) and Del/+ (n=10)] of our second model were analyzed separately from the observation of different events in pairs. The Del/+ male rat showed increased solitary time [Student's t-test: $t_{(18)}$=−2,229; p=0.039] and approaching behavior [Student's t-test $t_{(19)}$=−2,679; p=0.015]. No altered social behavior has been detected in females (*p<0.05; **p<0.01; ***p<0.001).

several groups with a higher number of upregulated pathways compared to the Del/+ model, as synaptic meta-pathway, signaling or transcription and epigenomic regulation, many downregulated pathways were observed in the Del/+ model, except the "transcription and epigenomic regulation" meta-pathway not being affected. Moreover, as expected from the DEA analysis, we indeed were able to identify 23 pathways that were commonly shared and upregulated in both Del/+ and Dup/+ (Figure 5B) with most of them being related to morphogenesis with the primary cilium, and four others unrelated. Oppositely "synaptic and Synaptic: other pathways" and "metabolism" functions were more affected in the Del/+ condition, while "transcription and epigenomic regulation" or "hormone regulation" were more perturbed in the Dup/+ model (Figures 5A,C).

3.4. CUL3 and MAPK3 functional subnetworks are central to the 16p11 dosage susceptible regulatory protein–protein interaction network

Then, we built the rat 16p11 dosage susceptible regulatory protein–protein interaction network (RegPPINet; Figure 6A) using as seeds all the genes identified by gage as altered in the Del/+ and/or in the Dup/+ SD models. We aimed to gain some insights into the possible molecular mechanism altered due to the gene dosage of the region. After performing the betweenness centrality analysis and analyzing the topology of the most central network we identified 47 main hubs. Several of those hubs involved genes from the region (Figure 6A) and interestingly we identified a few central genes linked to synaptic deregulation, re-enforcing the fact that synaptic dysfunction was one of the main alterations due to the dosage change of 16p11. These most important hubs in terms of betweenness were *Chd1, Gli1, Plg, Coro1a, Epha8, Disc1, Spag6l, Cfap52 or Sema3a.* However, if we consider the most connected gene, by the sole degree of regulatory interactions, then the 16p11 dosage RegPPINet pointed to Mapk3 and Cul3 (Figures 6B,C). The first subnetwork is centered on *Mapk3* with expressed genes also found altered in both Del/+ and Dup/+ models with opposite regulatory senses (like *Cdh1* or *Mvp*). In addition, we found 3 genes on this subnetwork, *Gdnf, Gata4* and *Atp1a4* downregulated in both models and one gene *Itgb6* upregulated in both. The *Cul3* network involved several genes whose expression was found altered in both Del/+ and Dup/+ models with mirroring regulatory effects for *Kctd13, Doc2a, Kif22, Rad21l1, Ppp4c* or *Asphd1*.

3.5. Proteomics analyses further support the major relevance of 16p11 gene dosage and the central role of MAPK3 and CUL3 interactors

Then, we wondered how much of the 16p11 dosage susceptible network could be confirmed by a quantitative proteomics analysis based on the hippocampus. Seven out of the 32 proteins encoded in the 16p11.2 region, were detected and successfully quantified by mass-spectrometry in the samples analyzed. Their expression profiles showed a clear correlation with gene dose with lower expression in Del/+, intermediated expression in wt and Del/Dup genotype, and higher expression in Dup/+. Dup/Del values followed partially the wt abundance (Supplementary Figure S5). There were 3 missing measures for Bola2, and D4A9P7 in the Del/+ group, which were very likely linked to low/borderline abundance in the samples.

Interestingly, most of the genes, contributing to the functional alteration in the 16p11 dosage and the transcription network, were also detected and quantified by the proteomic technique (highlighted in yellow with an octagonal shape; Supplementary Figure S6A). We found a strong correlation between the RNA level (RNA seq count) and our proteomic quantification in wt and Del/+ individuals for all expressed genes (Supplementary Figure S6B) and DEGs (Supplementary Figure S6C). Thus, we decided to investigate the proteomics dataset on its own and search for new insights into the 16p11 syndrome alterations. We built the proteomic-specific hippocampi 16p11 MinPPINet (Supplementary Figure S7A). Very well-connected 16p11 region proteins, such as ALDOA, BOLA2, CDIPT and COROA1, unraveled the existence of two main subnetworks (Supplementary Figure S7B): the first was around MAPK3 and SRC, a proto-oncogene coding for a membrane-bound non-receptor tyrosine kinase, while the second was built around the ATP citrate lyase (ACLY). ACLY is associated through the proteasome subunit, alpha type, 4 (PSMA4), to superoxide dismutase 1 (SOD1) and CUL3 for polyubiquitination and degradation of specific protein substrates.

3.6. Sexual dysmorphism observed at the transcriptomics level in 16p11 LE deletion models

Then we wonder if the rat's genetic background can also change major transcriptomics outcomes and if any sexual dysmorphism can

10.3389/fnins.2023.1148683

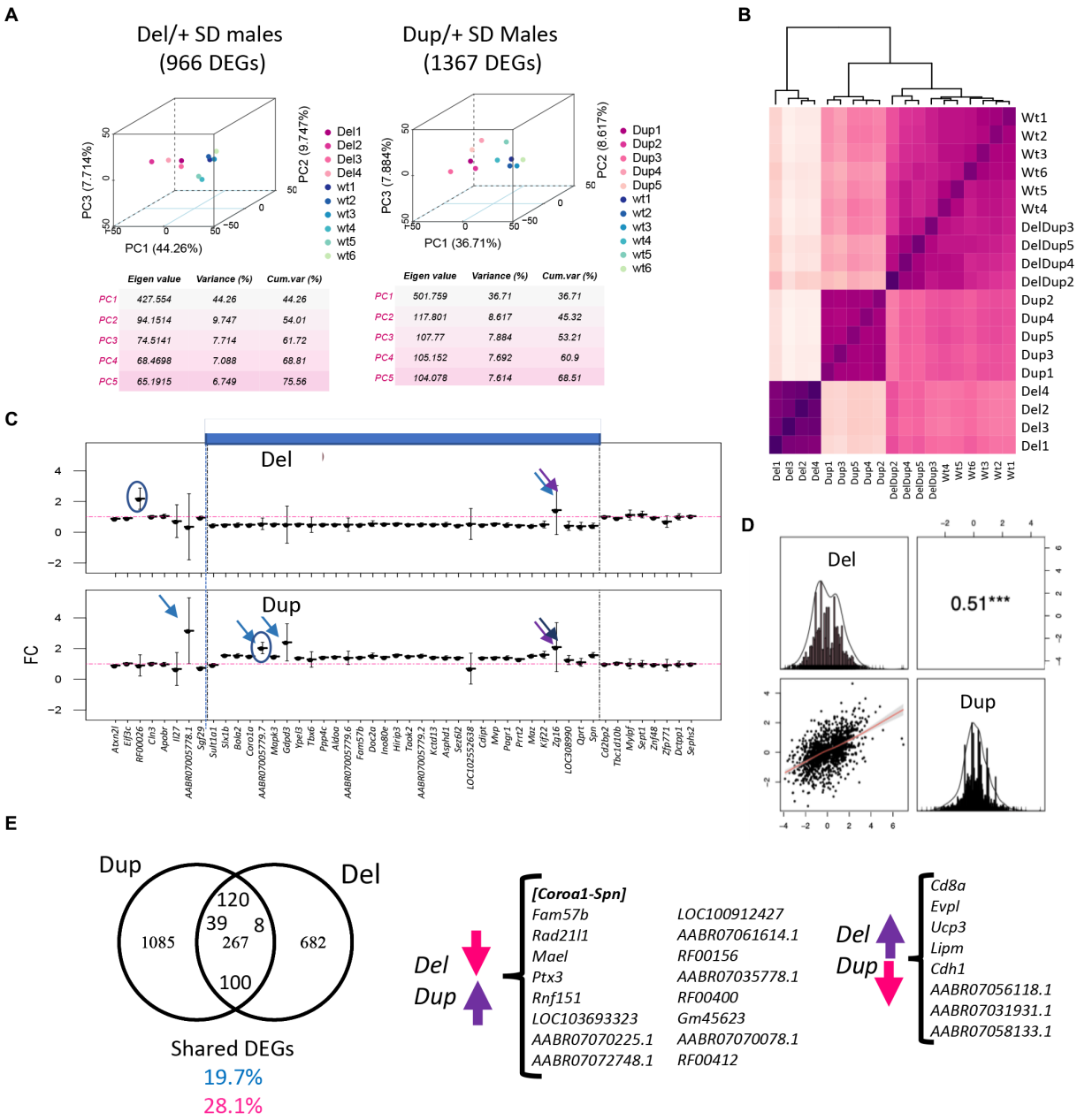

FIGURE 4
Gene expression analysis at the transcriptome and proteome level in the 16p11Del and Dup male rat hippocampi. **(A)** 3D principal component analysis (PCA) on the DEGs for each adult hippocampal sample allows for isolating the animals carrying the 16p11.2 deletion (Del/+) and the animals with the 16p11 region (Dup/+) in comparison with the wild-type littermates. From disomic (wt) adult hippocampi. **(B)** Homogeneity plot showing the gene dosage effect of the 28 genes in the 16p11.2 region and how the samples cluster by Euclidian distance. **(C)** Fold change expression levels of the genes analyzed by RNA-Seq homologous to the 16p11.2 region in rat chromosome 1 (Rno1). The genes are displayed following the order of their genomic start site coordinates. The 16p11.2 interval is indicated in blue. **(D)** Distribution and correlation diagram showing the DEGs in common between Del and Dup models and the model-specific DEGs. The shared DEGs correspond to 19.7% and 28.1% of the total DEGs identified, respectively, for the Dup and Del models. **(E)** Venn diagram showing in the left panel, the DEGs in common between the SD Del and Dup/+ models and SD male transcriptomics datasets and the background-specific DEGs. Highlighted inside the common genes those upregulated in both models, 120, downregulated in both 100 and regulated in opposing regulatory sense between Dup/+ and Del/+ models (39 upregulated in Dup/+ and 8 downregulated in Dup/+).

be detected. Thus, we isolated hippocampi from 5 females and 5 males Long Evans Del/+ and controlled wild-type littermates to carry out transcriptome analysis. The DEA analysis using FCROS identified 1,068 and 1,324 genes specifically dysregulated (DEGs) in Del/+ males and females, respectively (Table 1). Moreover, 1,544 DEGs were altered independently of the sex when we ran the analysis pooling both sexes together (Figure 7A). The computed PCA and the Euclidian distance matrix clustered the samples by their genotypes and then sex (Figure 7B). Moreover, the specific fold change of the 16p11.2 region in both males and females showed the expected downregulation in both sexes, similar to the one observed in the male SD Del/+ male model (Figure 7D). A good correlation occurred with the normalized

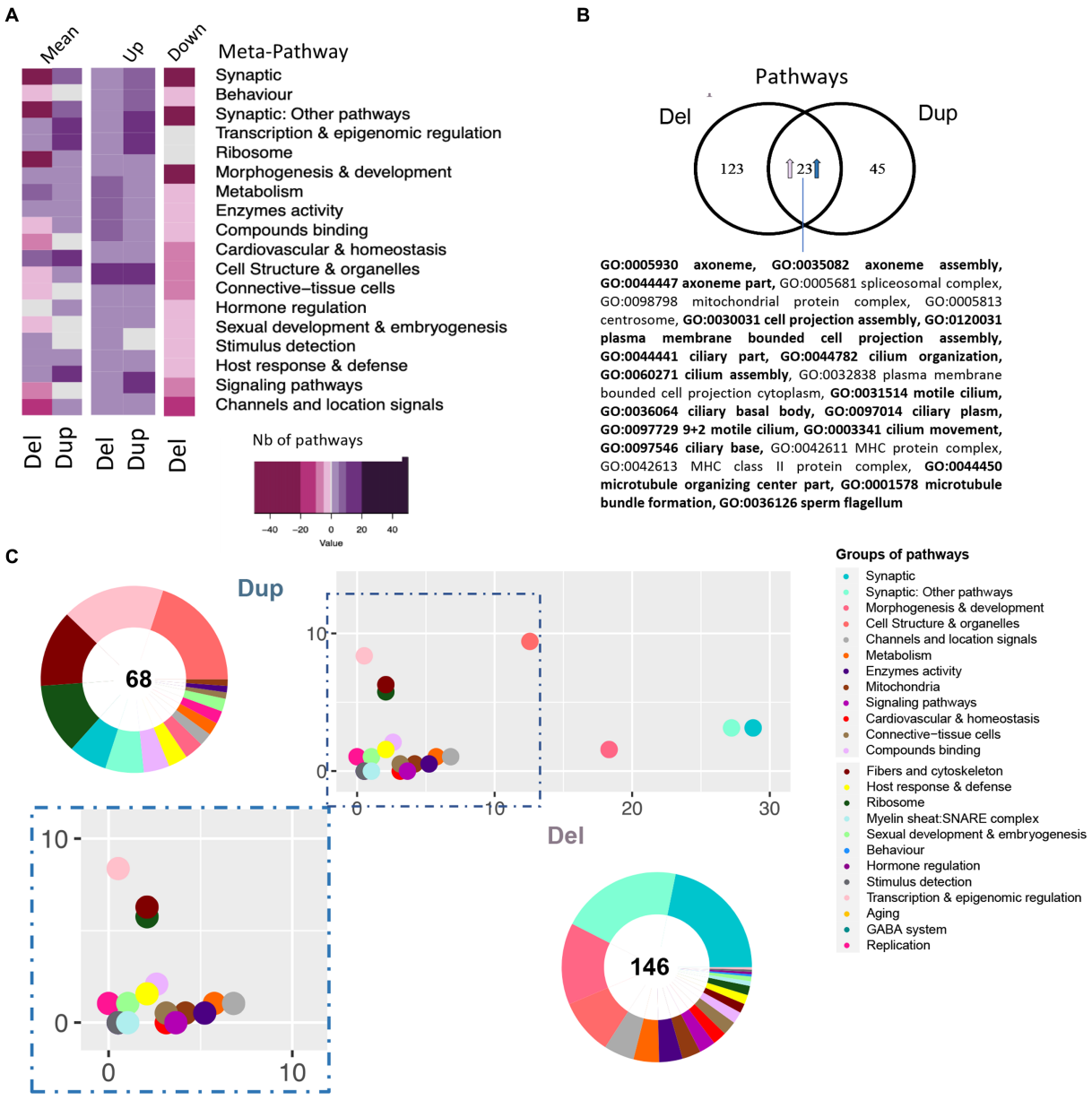

FIGURE 5
Pathway analysis of 16p11.2 SD rat Del and Dup male model based on the transcriptome of the hippocampi. **(A)** Heatmap representation of the number and regulation sense of the pathways of the Del and Dup models. Pathways identified using the GAGE R package and filtered by q-value cut-off < 0.1, were grouped in the meta-pathways shown on the ordinate. The color key represents the number of pathways within the meta-pathways 50, 20, 10, 5, 0. The minus or pink color represents downregulated pathways, the white color represents no pathway found in the meta-pathway and the purple or positive numbers stand for upregulated pathways, respectively. **(B)** Venn diagram highlighting the 23 pathways upregulated in both models and the existence of model-specific functional alteration. The percentage of shared pathways reached 33% or 15% of the total altered pathways in the Dup(16p11) and Del(16p11) models, respectively. Seventeen of those pathways are also found dysregulated in Del/Dup (in bold). **(C)** Ratio plot showing the inter-model comparison of the percentage of pathways included on each meta-pathway (group of pathways) normalized by the total number of unique pathways per meta-pathway. The x-axis and y-axis represent the SD male Del and Dup data, respectively. Outside a doughnut plot represented in the center, the number of total altered pathways found by gage analysis on each dataset and the percentage of pathways altered included on each meta-pathway is represented on the coronal area under each meta-pathway. The meta-pathways are defined in the accompanying legend.

counts of 16p11 region genes for wt and Del/+ genotypes in both LE male and female hippocampi (for wt $R^2 = 0.9996$, Del/+ $R^2 = 0.9988$) and also when comparing wt and Del/+ genotypes in males from the SD and LE genetic backgrounds (for wt $R^2 = 0.9966$, Del/+ $R^2 = 0.9987$; Supplementary Figure S8). Four genes from the region were confirmed by ddPCR to follow the dosage effect with lower expression in the Del/+ rat males and females compared to wt littermates. There was a limited number of DEGs commonly deregulated in both sexes compared to hippocampal DEGs specific for males and females and more DEGS were observed in males than in females (Figure 7C), suggesting that there was a strong influence of the sex on the genomic dysregulation induced by the deletion.

Sexual dysmorphism was also found at the level of the altered pathways. With 248 pathways altered in males and 100 identified in

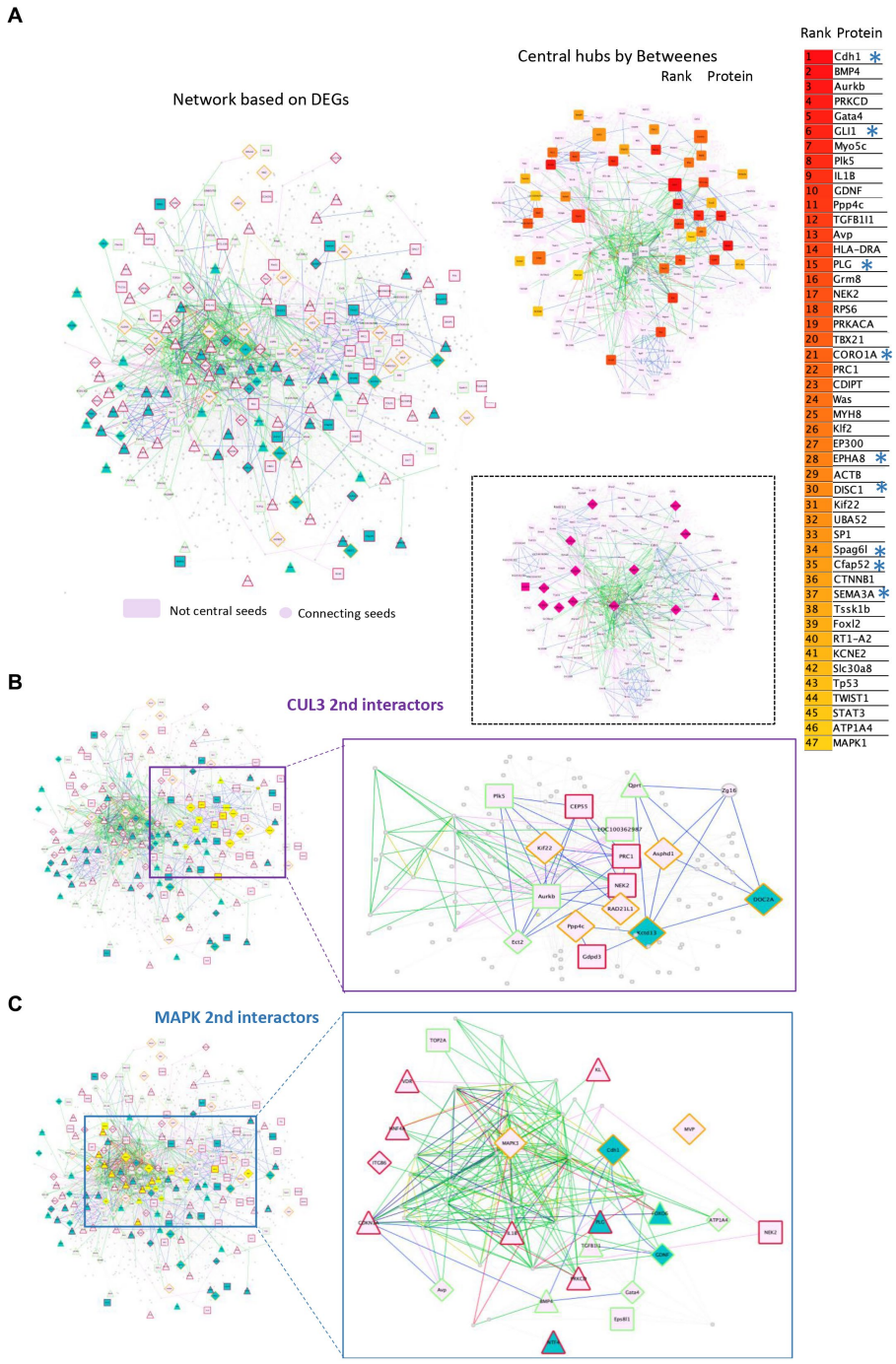

FIGURE 6
Protein–protein interaction networks altered due to the gene dosage effect based on the transcriptome analysis of the 16p11 SD rat models. **(A)** Left panel, a full rat protein–protein interaction network (RegPPINet) built using as seeds all the genes identified by gage as altered in the Del or Dup SD models visualized using the edge weighed spring embedded layout by betweenness index in Cytoscape. On the right panel, highlighting the main central nodes of the rat dosage susceptible RegPPINet network. On the bottom panel, highlight in pink the 16p11 region genes. The full RegPPINet was built by querying STRING and selecting the PPIs with a medium confidence score (CS=0.4) coming from all sources of evidence. The shapes of the nodes represent the following information: Shapes: (i) Pallid pink ellipses: represent connecting proteins added to assure the full connectivity of the network; Then the genes identified by GAGE after q-Val < 0.1 cut-offs to be contributing even slightly, to any pathway alteration and also identified in the DEA analysis by Fcros. The top 50 central genes are listed on the right side with genes known to be involved in synaptic pathways (*). **(B)** Second-level interactors of CUL3 were extracted from the main network. The left panel shows in yellow all the genes that are second-level interactors of CUL3. On the right panel, the extracted subnetwork centered around CUL3 to identify the molecular regulatory mechanisms known to exist between the interacting partners. **(C)** We extracted from the rat RegPPINet the second-level interactors of MAPK family proteins (proteins MAPK 1,3,8,9,14). Left panel, the full RegPPINet network can be observed highlighting in yellow all the genes that are second-level interactors of CUL3. On the right panel, the extracted subnetwork centered around MAPK proteins to identify the molecular regulatory mechanisms known to exist between the interacting partners. The shapes of the nodes represent the following information: Shapes: (i) Pallid pink ellipses: represent connecting proteins added to assure the full connectivity of the network; Then the genes identified by GAGE after q-Val < 0.1 cut-offs to be contributing even slightly, to any pathway

(Continued)

FIGURE 6 (Continued)

alteration and also identified in the DEA analysis by Fcros. Rectangles represent genes identified uniquely in Dup transcriptomes while triangles are for genes identified uniquely in Del transcriptomes and diamond shapes for genes identified as DEGs in both models. The edges color represent the type of interaction annotated by following the PathPPI classification (Tang et al., 2015), and ReactomeFIViz annotations as follows (i) The GErel edges indicating expression were colored in blue and repression in yellow. (ii) PPrel edges indicating activation were colored in green, inhibition in red. (iii) Interactions between proteins known to be part of complexes in violet. (iv) Predicted interactions were represented in gray including the PPI interactions identified by STRING DB (Szklarczyk et al., 2017) after merging both networks. The nodes bordering color represent If the gene was found upregulated in both models (red), downregulated in both (green) or in the mirroring regulatory sense (orange).

females, only 49 specific pathways were found deregulated in both sexes but only 2 followed the same regulatory sense (Figure 7C). We then used the classification in meta-pathways (Duchon et al., 2021) to better understand the changes associated with the deletion. Looking at the resulting component, some meta-pathway like "Synaptic," and "Synaptic: other pathways" were found downregulated in males while the resulting component was upregulated in females. Oppositely, "Behaviour," "Host & immune response," and "Morphogenesis and development" were found downregulated in males whereas those were upregulated in females (Figures 7E–F). Other meta-pathways were only found affected in Del/+ males. "Mitochondria" were only found upregulated in males while "hormone regulation" and "sexual development and embryogenesis" were downregulated only in males with no alteration in female carriers (Figures 7E–F). Overall, the alteration of pathways appeared to be more pronounced in males than in females.

Looking into the number of DEGs and pathways shared and unique in both SD and LE genetic backgrounds, we identified 182 common genes, most of them following the same regulatory sense and 48 pathways, 28 upregulated and 20 downregulated in both models (Figure 8A). Moreover, even though the number of total pathways altered in LE was higher than in SD (248 and 146 respectively) when looking at the proportion of pathways grouped on each meta-pathway considering the total number of unique pathways altered in both models only an important increase in "Cell structure" meta-pathway in LE compared to SD could be highlighted (Figure 8B). Considering the results obtained, we identified similar changes in the meta-pathways profiles pointing to the existence of a conserved and robust functional alteration profile (Figure 8C), mirrored in most of the meta-pathways in the Dup/+ model. Overall the main meta-pathways for synapse ("synaptic" and "synaptic other pathways") were commonly altered in the Del/+ models.

The few functional changes between the two genetic backgrounds were in "Apoptosis & cell death" and "post-translational modifications" which were only found affected in the LE background.

4. Discussion

In the present study, we described the first behavioral and cognitive phenotypes of 16p11.2 deletion and duplication of new rat models on SD and LE genetic backgrounds. A cognitive deficit was found in the novel object recognition memory test with 3 objects, and a defect in social interaction was observed with increased isolation behavior, a typical autistic trait, in 16p11.2 *Del*/+ males. The deletion of the *Sult1a1-Spn* region was also associated with the appearance of increased pinning events, a behavior considered an expression of dominance. In addition, this type of behavior could also be seen among pseudo-disomic *Del/Dup* carriers, suggesting a genetic construct effect not related to the dosage of genes from the region. This phenomenon may result from the new deletion allele that could alter the expression of neighboring genes. Besides, 16p11.2 duplication in males was linked to an increase in aggressiveness. These phenotypes could be associated with autistic traits and psychotic symptoms identified in patients affected by 16p11.2 rearrangements (Niarchou et al., 2019).

Interestingly in both outbred genetic backgrounds, the social and cognitive phenotypes were more noticeable in males than Del/+ females. The characterization of these models on a non-consanguineous genetic background allowed us to observe initially a large phenotypic variability compatible with the large symptomatic variability and the low penetrance of the neuropsychiatric disorders associated with CNVs 16p11.2 in humans. But it is important to emphasize that higher variability in the behavior outcome of phenotypic analysis hinders our research. We have used 8 cohorts of rats to increase the number of animals (about 20–25 animals per experiment) to be able to gather a larger part of the population. For these reasons, we consider it pertinent to analyze the robustness of the phenotypes associated with the 16p11.2 deletion (CNV that has caused a more severe phenotype in the SD model) through the new rat models with outbred genetics.

While in the SD model, the variability of behavior between individuals only allowed us to observe a trend of hyperactivity, in the new LE model we could corroborate a decrease in variability and the significant presence of hyperactivity and repetitive behaviors in males. In addition, we again detected a cognitive disorder in object recognition memory in males of the LE model, confirming the robustness of this phenotype in the 16p11.2 deletion syndrome.

Finally, when analyzing the social behavior of the LE model, we were also able to confirm the association of solitary behavior phenotype with the deletion of the genetic interval in males. Although there were direct contact events between the tested animals, these rats avoided the behavior of staying close to each other while exploring the test. This is a very common practice among rats, unlike mice tend to be more solitary, which makes rats more sociable beings and animal models most useful for the study of social disorders. In addition, curiously, we discovered that these animals spent more time approaching their test partner, which could be interpreted as cautious or scary behavior to approach an unknown animal.

In this area also, we again observed a greater sensitivity of the male sex or a greater resilience of the female sex to the deletion of the 16p11.2 region in this new genetic background. This phenomenon is also observed in humans where more males are affected by ASD than females in the population. Our observation supports the theory of Empathy-Systematization, according to which sexual psychological differences reflect a reinforcement of systematization in the male and

10.3389/fnins.2023.1148683

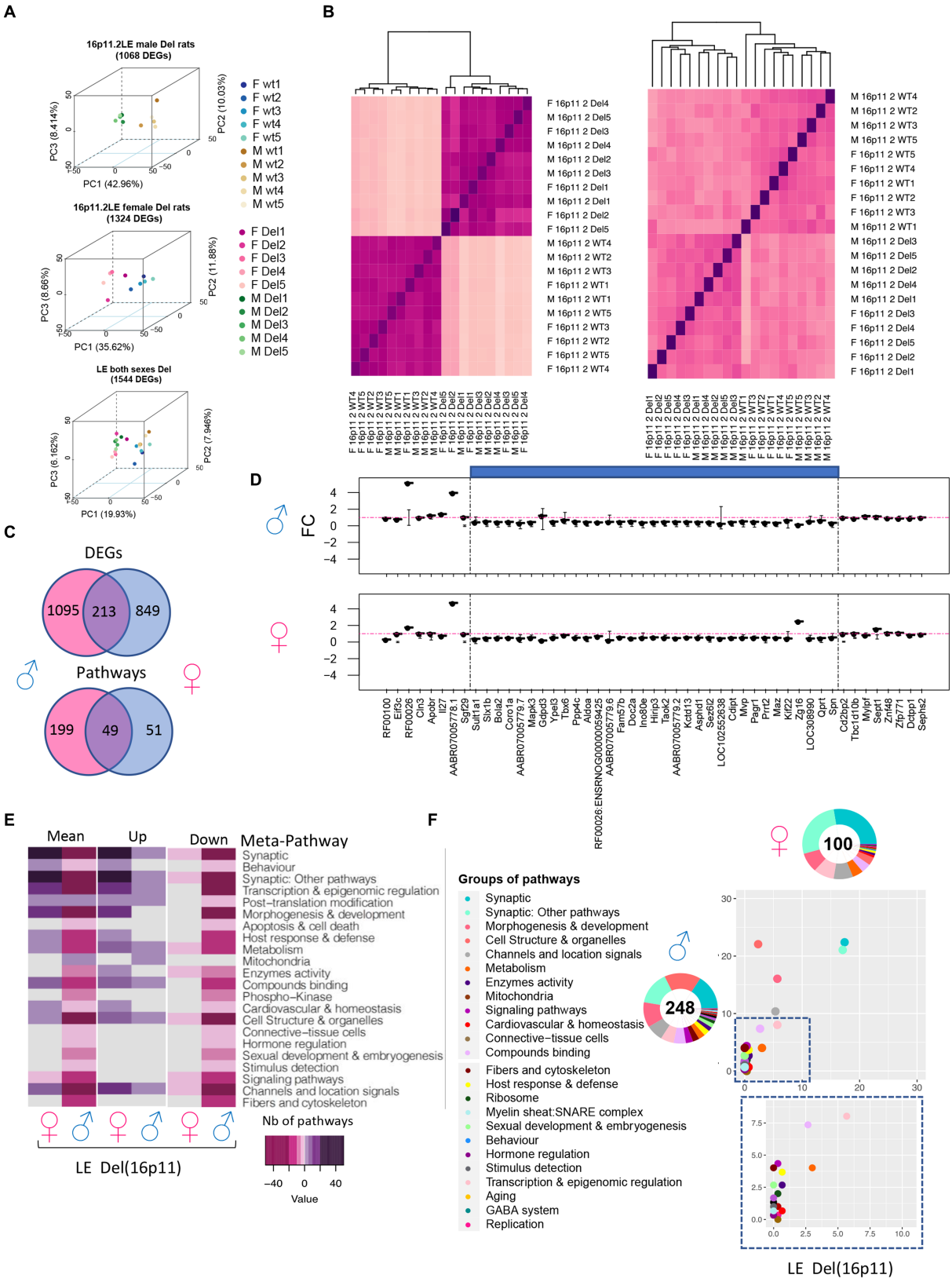

FIGURE 7
Gene expression analysis of 16p11 LE Del and control littermate (wt) male and female rats. **(A)** 3D-PCA on the DEGs for each adult hippocampal sample allows us to isolate the LE rats carrying the 16p11.2 deletion (Del) in comparison with the wild-type littermates in both sexes as shown in the upper and middle plots. As shown in the bottom plot even though there are some differences by sex the genotype effect is the major difference between the animals and its variability is explained in the first component "PC1." **(B)** Homogeneity plot showing the gene dosage effect of (left) the 28 genes in the 16p11.2 region and how the samples cluster by Euclidian distance, and (right) all DEGs identified in both male and female datasets. **(C)** Venn diagram

(Continued)

FIGURE 7 (Continued)

showing in the upper panel, the DEGs were found common between the male and female LE datasets. The shared DEGs correspond to 16.2% and 20% of the total DEGs identified, respectively, for female and males. In the bottom panel, the Venn diagram shows the pathways in common between the male and female LE datasets. The shared pathways correspond to 19.7% and 49% of the total pathways identified. **(D)** Fold change expression levels of the genes from the region homologous to 16p11.2 in Rno1. The genes are displayed following the order of their genomic start site coordinates. The deleted areas for each model appear shaded in blue. **(E)** Group of meta-pathways showing up or downregulation with a color key corresponding to the number of pathways within the meta-pathways. **(F)** Ratio plot showing the inter-model comparison of the percentage of pathways included on each meta pathway normalized by the total number of unique pathways per meta-pathway. The x-axis and y-axis represent the female and male data, respectively. Outside a doughnut plot representing in the center the number of total altered pathways found by gage analysis one each dataset and the percentage of pathways altered included on each meta-pathway is represented on the coronal area under each meta-pathway. The metapathways are defined in the legend.

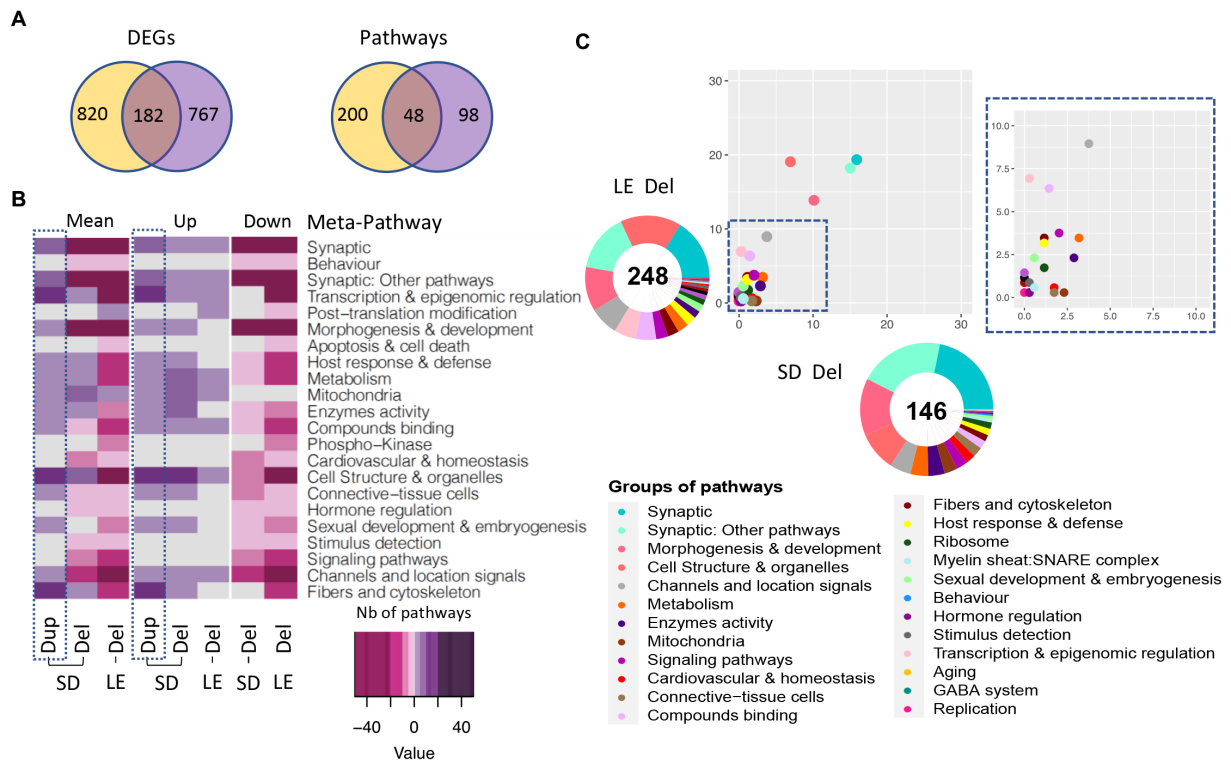

FIGURE 8
Gene expression analysis of the males LE vs. SD Del (16p11) rat models. **(A)** Venn diagram showing in the left panel, the DEGs in common between the LE and SD male transcriptomics datasets and the background-specific DEGs. The shared DEGs correspond to a 16.2 and 20% of the total DEGs identified, respectively, for the Dup and Del models. **(B)** Heatmap representation of the number and regulation sense of the pathways altered in the male rat from SD Del, SD Dup and LE Del models. **(C)** Ratio plot showing the inter-model comparison of the percentage of pathways included on each meta-pathway, normalized by the total number of unique pathways per meta-pathway. On the x-axis and y-axis represent the rat male SD Del and LE Del data, respectively. Outside a doughnut plot representing in the center the number of total altered pathways found by gage analysis for each dataset and the percentage of pathways altered included on each meta-pathway is represented on the coronal area under each meta-pathway.

a reinforcement of empathy in the female. In the context of TSA, this theory has an extension, called the "extreme male brain" according to which individuals are characterized by deficiencies in empathy with an intact or increased systematization (Baron-Cohen et al., 2005, 2011). Our data are also consistent with the proportion of identifying 16p11.2 rearrangements favorable for boys compared to girls reported in a previous study. This paper indicated a male: female ratio of 1.3:1 for the 16p11.2 deletion in autistic individuals and 1.6: 1 for the 16p11.2 deletion in patients with intellectual disability / developmental delay (Polyak et al., 2015). Further studies are needed for a better understanding of the mechanisms underlying risk and resilience to disease between the sexes.

Besides, we decided to evaluate the effect of 16p11.2 CNVs on the body weight of our rat models. Our study demonstrates that the deletion of the genetic interval causes only a significant reduction in body weight of young mutant males on SD background. However, for the LE model, we decided to measure the body weight of our animals at three different moments of their development. We were able to verify that the 16p11.2 deletion also causes a decrease in the weight of the mutant males at three ages, but the female sex seems to start with a normal body weight and suffer a significant loss throughout its development. These results are in line with the characterization of 16p11.2 mouse models (Arbogast et al., 2016). However, in our rat model, the male rats carrying 16p11.2 duplication do not show a

phenotype. On the other hand, considering the results obtained in the phenotypic study of the mouse and rat model, as opposed to the symptoms diagnosed in patients, we could hypothesize that the effect of 16p11.2 BP4-BP5 CNVs on body weight may be a specificity of the human species.

The gene expression analysis of mRNA isolated from adult rat hippocampi in SD 16p11.2 Del/+ and Dup/+ models demonstrated that 23 pathways were commonly shared and mis-regulated in both Del/+ and Dup/+. In the 16p11.2 rat models, the pathway around the primary cilium was also found altered; as described previously in mice (Migliavacca et al., 2015). Other changes found in the Del/+ pathways were mirrored to some extent in the Dup/+ but the severity of the changes varied between the two conditions. In addition, several additional pathways were different confirming diverse effects induced by the Del/+ and the Dup/+, as found in the mouse models (Arbogast et al., 2016). One of the main alterations due to the dosage change of 16p11 was linked to the synapses, with the main central genes not linked to the regions: *Chd1, Gli1, Plg, Epha8, Disc1, Spag6l, Cfap52 or Sema3a,* except *Coro1a;* Six of which, *Chd1, Gli1, Plg, Disc1, Sema3a and Coro1a,* are reported to "abnormality of the nervous systems" in the Human Phenome Ontology. Interestingly, the most connected genes highlighted the MAPK3 and CUL3 subnetworks in the 16p11.2 models. MAPK3 is a gene from the 16p11.2 interval, thus subjected to change in dosage, and involved in the 16p11.2 syndromes (Pucilowska et al., 2015, 2018) whereas CUL3 is a target of KCTD13, another gene of the 16p11.2 region, controlling the RHOA pathway perturbed in 16p11.2 models (Lin et al., 2015; Martin Lorenzo et al., 2021). Both molecular pathways were also pointed in the proteomic studies, linked, respectively, with other proteins like SRC and ACLY.

Using the analysis of both sexes in the LE 16p11.2 Del model, we identified more DEGs in the male mutant hippocampi compared to females; DEGs that were also found in the SD genetic background. Of the 248 pathways altered in the Del/+ males and 100 identified in mutant females, 49 pathways were found deregulated in both sexes. More effects were observed in males than in females in various pathways, including the synapse, the Behavior, and mitochondria. By introducing the known gene/phenotype associations, described in the DisGeNet, GO and Kegg databases, we identified *Prrt2* as a candidate gene involved in "aggressively and stereotyped behaviour" that was found upregulated in the Dup/+ model and downregulated in Del/+. We also found 4 other genes from the 16p11.2 region involved in autistic behavior (defined by increased time in isolation) downregulated in Del and upregulated in Dup/+: *Taok2, Kctd13, Sez6l2, Mapk3*. The last two are also found in the proteomics analysis as differentially quantified peptides (Eps). Similarly, we found several genes linked to increasing time in isolation only upregulated in the Del/+ model as *Glp1r, Sema3a* or *Disc1*. Next, we wondered if we could identify any gene potentially responsible for the hypoactivity phenotype observed in the Dup model and we found 9 genes: *Coro1a*, Kctd13, Sez6l2, Spn, Aldoa, Mapk3*, Cdh1, Doc2a* and *Prrt2*. Finally, we identified 4 genes, namely *Eps*, *Prrt2, Mapk3,* and *Cdh1,* linked to memory and cognition deficits observed in the Del/+ model carriers and with mirroring regulatory sense in Dup/+ individuals.

Overall, the two new rat models for the 16p11.2 syndromes described here are promising in terms of behavior alteration with more social phenotypes and similar molecular pathways, MAPK2 and KCTD13/CUL3/RHOA affected in the rat brain compared to the mouse. We already described some craniofacial changes in the SD 16p11.2 models close to the human features (Qiu et al., 2019). Nevertheless, further explorations are needed to explore the variety of phenotypes related to humans as it is currently done in the mouse. More in-depth social behavior analysis (Rusu et al., 2022) provides a more detailed description of social impairment and a strong quantitative approach is crucial to pursue if we wish 1 day to test a drug that can mitigate the social impairment observed in the 16p11.2 syndromes.

Data availability statement

The datasets presented in this study can be found in online repositories. The GEO online repositories (Accession No. GSE225135).

Ethics statement

The animal study was reviewed and approved by Com'Eth N°17.

Author contributions

YH: conceptualization. SMa, MM, and WR: data curation. MM, VN, and WR: formal analysis. YH and LN: funding acquisition. SMa, HA, MP, LL, LN, and VN: investigation. J-PC, SMe, IA, M-CB, and YH: methodology. M-CB, IA, and YH: project administration. SMe, LT, GP, IA, and WR: resources. MM and WR: software. IA, J-PC, LN, M-CB, and YH: supervision. SMe, GP, IA, M-CB, LN, WR, and YH: validation. SMa, MM, WR, and YH: visualization. SMa, MM, and YH: writing—original draft preparation. SMa, MM, HA, MP, VN, WR, GP, LL, M-CB, SMe, LT, LN, J-PC, IA, and YH: writing—review and editing. All authors contributed to the article and approved the submitted version.

Funding

This work was supported by a grant from the Simons Foundation (SFARI 548888 to YH) and by the National Centre for Scientific Research (CNRS), the French National Institute of Health and Medical Research (INSERM), the University of Strasbourg (Unistra), French government funds through the "Agence Nationale de la Recherche" in the framework of the Investissements d'Avenir program by IdEx Unistra (ANR-10-IDEX-0002), a SFRI-STRAT'US project (ANR 20-SFRI-0012), "TEFOR" "Investissements d'Avenir" (ANRIIINSB-0014), EUR IMCBio (ANR-17-EURE-0023), and INBS PHENOMIN (ANR-10-IDEX-0002-02) and also provided to the GenomEast platform, a member of the "France Génomique" consortium for the RNASeq processing (ANR-10-INBS-0009), and to the Proteomic platform of IGBMC, that was supported by an ARC foundation grant (Orbitrap) and a Canceropole Grand Est foundation grant. The funders had no role in the study design, data collection and analysis, decision to publish, or preparation of the manuscript.

Acknowledgments

We would like to thank the members of the research group, the IGBMC laboratory and of the ICS for their help in brain morphometric analysis. We extend our thanks to the animal caretakers of the ICS who are in charge of the mice's well-being.

Conflict of interest

The authors declare that the research was conducted in the absence of any commercial or financial relationships that could be construed as a potential conflict of interest.

Publisher's note

Supplementary material

The Supplementary material for this article can be found online at: https://www.frontiersin.org/articles/10.3389/fnins.2023.1148683/full#supplementary-material

References

Angelakos, C. C., Watson, A. J., O'brien, W. T., Krainock, K. S., Nickl-Jockschat, T., and Abel, T. (2017). Hyperactivity and male-specific sleep deficits in the 16p11.2 deletion mouse model of autism. *Autism Res.* 10, 572–584. doi: 10.1002/aur.1707

Arbogast, T., Ouagazzal, A.-M., Chevalier, C., Kopanitsa, M., Afinowi, N., Migliavacca, E., et al. (2016). Reciprocal effects on neurocognitive and metabolic phenotypes in mouse models of 16p11.2 deletion and duplication syndromes. *PLoS Genet.* 12:e1005709. doi: 10.1371/journal.pgen.1005709

Ashburner, M., Ball, C. A., Blake, J. A., Botstein, D., Butler, H., Cherry, J. M., et al. (2000). Gene ontology: a tool for the unification of biology. The gene ontology consortium. *Nat. Genet.* 25, 25–29. doi: 10.1038/75556

Baron-Cohen, S., Knickmeyer, R. C., and Belmonte, M. K. (2005). Sex differences in the brain: implications for explaining autism. *Science* 310, 819–823. doi: 10.1126/science.1115455

Baron-Cohen, S., Lombardo, M. V., Auyeung, B., Ashwin, E., Chakrabarti, B., and Knickmeyer, R. (2011). Why are autism spectrum conditions more prevalent in males? *PLoS Biol.* 9:e1001081. doi: 10.1371/journal.pbio.1001081

Benedetti, A., Molent, C., Barcik, W., and Papaleo, F. (2022). Social behavior in 16p11.2 and 22q11.2 copy number variations: insights from mice and humans. *Genes Brain Behav.* 21:e12787. doi: 10.1111/gbb.12787

Chawner, S., Doherty, J. L., Anney, R. J. L., Antshel, K. M., Bearden, C. E., Bernier, R., et al. (2021). A genetics-first approach to dissecting the heterogeneity of Autism: phenotypic comparison of Autism risk copy number variants. *Am. J. Psychiatry* 178, 77–86. doi: 10.1176/appi.ajp.2020.20010015

Cooper, G. M., Coe, B. P., Girirajan, S., Rosenfeld, J. A., Vu, T. H., Baker, C., et al. (2011). A copy number variation morbidity map of developmental delay. *Nat. Genet.* 43, 838–846. doi: 10.1038/ng.909

D'Angelo, D., Lebon, S., Chen, Q., Martin-Brevet, S., Snyder, L. G., Hippolyte, L., et al. (2016). Defining the effect of the 16p11.2 duplication on cognition, behavior, and medical comorbidities. *JAMA Psychiat.* 73, 20–30. doi: 10.1001/jamapsychiatry.2015.2123

Dembélé, D., and Kastner, P. (2014). Fold change rank ordering statistics: a new method for detecting differentially expressed genes. *BMC Bioinformatics* 15:14. doi: 10.1186/1471-2105-15-14

Drakesmith, M., Parker, G. D., Smith, J., Linden, S. C., Rees, E., Williams, N., et al. (2019). Genetic risk for schizophrenia and developmental delay is associated with shape and microstructure of midline white-matter structures. *Transl. Psychiatry* 9:102. doi: 10.1038/s41398-019-0440-7

Duchon, A., Del Mar Muñiz Moreno, M., Lorenzo, S. M., De Souza, M. P. S., Chevalier, C., Nalesso, V., et al. (2021). Multi-influential genetic interactions alter behaviour and cognition through six main biological cascades in down syndrome mouse models. *Hum. Mol. Genet.* 30, 771–788. doi: 10.1093/hmg/ddab012

Esling, P., Lejzerowicz, F., and Pawlowski, J. (2015). Accurate multiplexing and filtering for high-throughput amplicon-sequencing. *Nucleic Acids Res.* 43, 2513–2524. doi: 10.1093/nar/gkv107

Fernandez, B. A., Roberts, W., Chung, B., Weksberg, R., Meyn, S., Szatmari, P., et al. (2010). Phenotypic spectrum associated with de novo and inherited deletions and duplications at 16p11.2 in individuals ascertained for diagnosis of autism spectrum disorder. *J. Med. Genet.* 47, 195–203. doi: 10.1136/jmg.2009.069369

Hastings, P. J., Lupski, J. R., Rosenberg, S. M., and Ira, G. (2009). Mechanisms of change in gene copy number. *Nat. Rev. Genet.* 10, 551–564. doi: 10.1038/nrg2593

Horev, G., Ellegood, J., Lerch, J. P., Son, Y. E., Muthuswamy, L., Vogel, H., et al. (2011). Dosage-dependent phenotypes in models of 16p11.2 lesions found in autism. *Proc. Natl. Acad. Sci. U. S. A.* 108, 17076–17081. doi: 10.1073/pnas.1114042108

Jacquemont, S., Reymond, A., Zufferey, F., Harewood, L., Walters, R. G., Kutalik, Z., et al. (2011). Mirror extreme BMI phenotypes associated with gene dosage at the chromosome 16p11.2 locus. *Nature* 478, 97–102. doi: 10.1038/nature10406

Karp, N. A., Meehan, T. F., Morgan, H., Mason, J. C., Blake, A., Kurbatova, N., et al. (2015). Applying the ARRIVE guidelines to an in vivo database. *PLoS Biol.* 13:e1002151. doi: 10.1371/journal.pbio.1002151

Kilkenny, C., Browne, W. J., Cuthill, I. C., Emerson, M., and Altman, D. G. (2010). Improving bioscience research reporting: the ARRIVE guidelines for reporting animal research. *PLoS Biol.* 8:e1000412. doi: 10.1371/journal.pbio.1000412

Lin, G. N., Corominas, R., Lemmens, I., Yang, X., Tavernier, J., Hill, D. E., et al. (2015). Spatiotemporal 16p11.2 protein network implicates cortical late mid-fetal brain development and KCTD13-Cul3-RhoA pathway in psychiatric diseases. *Neuron* 85, 742–754. doi: 10.1016/j.neuron.2015.01.010

Lindner, L., Cayrou, P., Jacquot, S., Birling, M. C., Herault, Y., and Pavlovic, G. (2021). Reliable and robust droplet digital PCR (ddPCR) and RT-ddPCR protocols for mouse studies. *Methods* 191, 95–106. doi: 10.1016/j.ymeth.2020.07.004

Lorbach, M., Kyriakou, E. I., Poppe, R., Van Dam, E. A., Noldus, L. P. J. J., and Veltkamp, R. C. (2018). Learning to recognize rat social behavior: novel dataset and cross-dataset application. *J. Neurosci. Methods* 300, 166–172. doi: 10.1016/j.jneumeth.2017.05.006

Love, M. I., Huber, W., and Anders, S. (2014). Moderated estimation of fold change and dispersion for RNA-seq data with DESeq2. *Genome Biol.* 15:550. doi: 10.1186/s13059-014-0550-8

Luo, W., Friedman, M. S., Shedden, K., Hankenson, K. D., and Woolf, P. J. (2009). GAGE: generally applicable gene set enrichment for pathway analysis. *BMC Bioinformatics* 10:161. doi: 10.1186/1471-2105-10-161

Marshall, C. R., Noor, A., Vincent, J. B., Lionel, A. C., Feuk, L., Skaug, J., et al. (2008). Structural variation of chromosomes in autism spectrum disorder. *Am. J. Hum. Genet.* 82, 477–488. doi: 10.1016/j.ajhg.2007.12.009

Martin Lorenzo, S., Nalesso, V., Chevalier, C., Birling, M. C., and Herault, Y. (2021). Targeting the RHOA pathway improves learning and memory in adult Kctd13 and 16p11.2 deletion mouse models. *Mol. Autism.* 12:1. doi: 10.1186/s13229-020-00405-7

Mccarthy, S. E., Makarov, V., Kirov, G., Addington, A. M., Mcclellan, J., Yoon, S., et al. (2009). Microduplications of 16p11.2 are associated with schizophrenia. *Nat. Genet.* 41, 1223–1227. doi: 10.1038/ng.474

Menoret, S., De Cian, A., Tesson, L., Remy, S., Usal, C., Boule, J. B., et al. (2015). Homology-directed repair in rodent zygotes using Cas9 and TALEN engineered proteins. *Sci. Rep.* 5:14410. doi: 10.1038/srep14410

Migliavacca, E., Golzio, C., Maennik, K., Blumenthal, I., Oh, E. C., Harewood, L., et al. (2015). A potential contributory role for ciliary dysfunction in the 16p11.2 600 kb BP4-BP5 pathology. *Am. J. Hum. Genet.* 96, 784–796. doi: 10.1016/j.ajhg.2015.04.002

Motulsky, H. J., and Brown, R. E. (2006). Detecting outliers when fitting data with nonlinear regression - a new method based on robust nonlinear regression and the false discovery rate. *BMC Bioinformatics* 7:123.

Nassar, L. R., Barber, G. P., Benet-Pagès, A., Casper, J., Clawson, H., Diekhans, M., et al. (2023). The UCSC Genome Browser database: 2023 update. *Nucleic. Acids Res.* 51, D1188–D1195.

Niarchou, M., Chawner, S. J. R. A., Doherty, J. L., Maillard, A. M., Jacquemont, S., Chung, W. K., et al. (2019). Psychiatric disorders in children with 16p11.2 deletion and duplication. *Transl. Psychiatry* 9. doi: 10.1038/s41398-018-0339-8

Polyak, A., Rosenfeld, J. A., and Girirajan, S. (2015). An assessment of sex bias in neurodevelopmental disorders. *Genome Med.* 7:94. doi: 10.1186/s13073-015-0216-5

Portmann, T., Yang, M., Mao, R., Panagiotakos, G., Ellegood, J., Dolen, G., et al. (2014). Behavioral abnormalities and circuit defects in the basal ganglia of a mouse model of 16p11.2 deletion syndrome. *Cell Rep.* 7, 1077–1092. doi: 10.1016/j.celrep.2014.03.036

Pucilowska, J., Vithayathil, J., Pagani, M., Kelly, C., Karlo, J. C., Robol, C., et al. (2018). Pharmacological inhibition of ERK signaling rescues pathophysiology and behavioral phenotype associated with 16p11.2 chromosomal deletion in mice. *J. Neurosci.* 38, 6640–6652. doi: 10.1523/JNEUROSCI.0515-17.2018

Pucilowska, J., Vithayathil, J., Tavares, E. J., Kelly, C., Karlo, J. C., and Landreth, G. E. (2015). The 16p11.2 deletion mouse model of Autism exhibits altered cortical progenitor proliferation and brain Cytoarchitecture linked to the ERK MAPK pathway. *J. Neurosci.* 35, 3190–3200. doi: 10.1523/JNEUROSCI.4864-13.2015

Qiu, Y., Arbogast, T., Lorenzo, S. M., Li, H., Tang, S. C., Richardson, E., et al. (2019). Oligogenic effects of 16p11.2 copy-number variation on craniofacial development. *Cell Rep.* 28:3320. doi: 10.1016/j.celrep.2019.08.071

Redaelli, S., Maitz, S., Crosti, F., Sala, E., Villa, N., Spaccini, L., et al. (2019). Refining the phenotype of recurrent rearrangements of chromosome 16. *Int. J. Mol. Sci.* 20:1095. doi: 10.3390/ijms20051095

Rees, E., Walters, J. T. R., Georgieva, L., Isles, A. R., Chambert, K. D., Richards, A. L., et al. (2014). Analysis of copy number variations at 15 schizophrenia-associated loci. *Br. J. Psychiatry* 204, 108–114. doi: 10.1192/bjp.bp.113.131052

Reinthaler, E. M., Lal, D., Lebon, S., Hildebrand, M. S., Dahl, H. H., Regan, B. M., et al. (2014). 16p11.2 600 kb duplications confer risk for typical and atypical Rolandic epilepsy. *Hum. Mol. Genet.* 23, 6069–6080. doi: 10.1093/hmg/ddu306

Rusu, A., Chevalier, C., De Chaumont, F., Nalesso, V., Brault, V., Hérault, Y., et al. (2022). A 16p11.2 deletion mouse model displays quantitatively and qualitatively different behaviours in sociability and social novelty over short- and long-term observation. bioRxiv [Preprint].

Sanders, S. J., Ercan-Sencicek, A. G., Hus, V., Luo, R., Murtha, M. T., Moreno-De-Luca, D., et al. (2011). Multiple recurrent de novo CNVs, including duplications of the 7q11.23 Williams syndrome region, are strongly associated with autism. *Neuron* 70, 863–885. doi: 10.1016/j.neuron.2011.05.002

Shinawi, M., Liu, P., Kang, S.-H. L., Shen, J., Belmont, J. W., Scott, D. A., et al. (2010). Recurrent reciprocal 16p11.2 rearrangements associated with global developmental delay, behavioural problems, dysmorphism, epilepsy, and abnormal head size. *J. Med. Genet.* 47, 332–341. doi: 10.1136/jmg.2009.073015

Steinberg, S., De Jong, S., Mattheisen, M., Costas, J., Demontis, D., Jamain, S., et al. (2014). Common variant at 16p11.2 conferring risk of psychosis. *Mol. Psychiatry* 19, 108–114. doi: 10.1038/mp.2012.157

Steinman, K. J., Spence, S. J., Ramocki, M. B., Proud, M. B., Kessler, S. K., Marco, E. J., et al. (2016). 16p11.2 deletion and duplication: characterizing neurologic phenotypes in a large clinically ascertained cohort. *Am. J. Med. Genet. A* 170, 2943–2955. doi: 10.1002/ajmg.a.37820

Szklarczyk, D., Morris, J. H., Cook, H., Kuhn, M., Wyder, S., Simonovic, M., et al. (2017). The STRING database in 2017: quality-controlled protein-protein association networks, made broadly accessible. *Nucleic Acids Res.* 45, D362–D368. doi: 10.1093/nar/gkw937

Tang, H., Zhong, F., Liu, W., He, F., and Xie, H. (2015). PathPPI: an integrated dataset of human pathways and protein-protein interactions. *Sci. China Life Sci.* 58, 579–589. doi: 10.1007/s11427-014-4766-3

Torres, F., Barbosa, M., and Maciel, P. (2016). Recurrent copy number variations as risk factors for neurodevelopmental disorders: critical overview and analysis of clinical implications. *J. Med. Genet.* 53, 73–90. doi: 10.1136/jmedgenet-2015-103366

Walters, R. G., Jacquemont, S., Valsesia, A., De Smith, A. J., Martinet, D., Andersson, J., et al. (2010). A new highly penetrant form of obesity due to deletions on chromosome 16p11.2. *Nature* 463, 671–675. doi: 10.1038/nature08727

Weiss, L. A., Shen, Y., Korn, J. M., Arking, D. E., Miller, D. T., Fossdal, R., et al. (2008). Association between microdeletion and microduplication at 16p11.2 and autism. *N. Engl. J. Med.* 358, 667–675. doi: 10.1056/NEJMoa075974

Zufferey, F., Sherr, E. H., Beckmann, N. D., Hanson, E., Maillard, A. M., Hippolyte, L., et al. (2012). A 600 kb deletion syndrome at 16p11.2 leads to energy imbalance and neuropsychiatric disorders. *J. Med. Genet.* 49, 660–668. doi: 10.1136/jmedgenet-2012-101203